

**Zeitschrift:** Schweizerische mineralogische und petrographische Mitteilungen = Bulletin suisse de minéralogie et pétrographie  
**Band:** 78 (1998)  
**Heft:** 1  
  
**Artikel:** REE geochemistry systematics of scheelite from the Alps using luminescence spectroscopy : from global regularities to local control  
**Autor:** Uspensky, Evgeny / Brugger, Joël / Graeser, Stefan  
**DOI:** <https://doi.org/10.5169/seals-59273>

### **Nutzungsbedingungen**

Die ETH-Bibliothek ist die Anbieterin der digitalisierten Zeitschriften auf E-Periodica. Sie besitzt keine Urheberrechte an den Zeitschriften und ist nicht verantwortlich für deren Inhalte. Die Rechte liegen in der Regel bei den Herausgebern beziehungsweise den externen Rechteinhabern. Das Veröffentlichen von Bildern in Print- und Online-Publikationen sowie auf Social Media-Kanälen oder Webseiten ist nur mit vorheriger Genehmigung der Rechteinhaber erlaubt. [Mehr erfahren](#)

### **Conditions d'utilisation**

L'ETH Library est le fournisseur des revues numérisées. Elle ne détient aucun droit d'auteur sur les revues et n'est pas responsable de leur contenu. En règle générale, les droits sont détenus par les éditeurs ou les détenteurs de droits externes. La reproduction d'images dans des publications imprimées ou en ligne ainsi que sur des canaux de médias sociaux ou des sites web n'est autorisée qu'avec l'accord préalable des détenteurs des droits. [En savoir plus](#)

### **Terms of use**

The ETH Library is the provider of the digitised journals. It does not own any copyrights to the journals and is not responsible for their content. The rights usually lie with the publishers or the external rights holders. Publishing images in print and online publications, as well as on social media channels or websites, is only permitted with the prior consent of the rights holders. [Find out more](#)

**Download PDF:** 16.09.2025

**ETH-Bibliothek Zürich, E-Periodica, <https://www.e-periodica.ch>**

# REE geochemistry systematics of scheelite from the Alps using luminescence spectroscopy: from global regularities to local control

by Evgeny Uspensky<sup>1</sup>, Joël Brugger<sup>2,3</sup> and Stefan Graeser<sup>2</sup>

## Abstract

Scheelite [CaWO<sub>4</sub>] is a common accessory mineral in various kinds of rocks and ore deposits. Rare earth elements (REE) geochemistry of ore minerals may give information about the source of the ore-bearing fluid, and about the physico-chemical conditions of ore transport and/or precipitation. Luminescence spectroscopy is able to detect several of the REE<sup>3+</sup> ions substituting for Ca<sup>2+</sup> in the scheelite lattice; however, difficulties in the interpretation of the luminescence spectra in terms of quantifying the REE prohibited the extensive use of luminescence as an analytical method for REE in scheelite.

This paper describes a new luminescence method, named thermal X-ray excited luminescence spectroscopy (XLT), which drastically increases the peak/background ratio in the luminescence spectra of scheelite. This method allows to analyse even small samples (single grains < 0.2 mm), is sensitive only to REE<sup>3+</sup> ions replacing Ca<sup>2+</sup> in the scheelite lattice (avoiding contamination e.g., by mineral inclusions), and is well suited for the analysis of large sample sets.

Our study concentrates on 70 samples of scheelite from the Alps, but draws on a yet unpublished database of more than 2000 scheelite spectra from 350 occurrences world-wide. This work demonstrates that luminescence spectra are a powerful tool in the discussion of diverse metallogenic problems, even if they are not converted to REE concentrations.

The luminescence spectra of scheelite exhibit several characteristic features which are diagnostic to the genetic type of the mineralisation. In particular, it is possible to distinguish scheelites from skarn/calcsilicate rocks, from molybdenite-veins, from stratabound metamorphic deposits, or from hydrothermal deposits. Scheelite from hydrothermal Au-deposits also often display distinctive characteristics.

Different case studies illustrate the ability of the XLT method to recognise hydrothermal events at the scale of an ore province. Applied to the study of single grains from heavy mineral concentrates obtained from fluvial sediments, the XLT method enables the genetic type of the lode deposit to be recognised, thus proving to be a promising prospecting tool.

**Keywords:** scheelite, Au-deposits, luminescence spectroscopy, geochemistry, REE, Alps.

## Introduction

In the last few decades the geochemistry of REE has been used with great success mainly in petrogenetic studies of igneous rocks. However, relatively few investigations are devoted to studies of REE in ore-forming systems (see LOTTERMOSER, 1992 and GIERÉ, 1996 for recent reviews). The REE pattern of a hydrothermal mineral is con-

trolled (i) at the source, by the nature of the REE reservoir; (ii) during transport, by the physico-chemical parameters of the fluid, including Eh, pH, T, and availability of ligands for REE complexation, and (iii) at the place of precipitation, by competition with other species and by the mechanisms of REE incorporation by the mineral, e.g., equilibrium (MORGAN and WANDLESS, 1980) or disequilibrium (RAKOVAN and REEDER, 1994) co-

<sup>1</sup> IGM of Russian Academy of Sciences, Staromonetny Per. 35, Moscow, 109017 Russia.

<sup>2</sup> Institute for Mineralogy and Petrography, University of Basel, Bernoullistr. 30, CH-4056 Basel, Switzerland.

<sup>3</sup> Present address: VIEPS, Department of Earth Sciences, Monash University, Clayton, Victoria 3168, Australia. <joelb@artemis.earth.monash.edu.au> (corresponding author).

precipitation, or sorption (KOEPPENKASTROP and DE CARLO, 1992). The applications of REE geochemistry to hydrothermal systems reflect the various nature of the controlling processes; thus, REE contents of hydrothermal minerals were used for example to monitor the source of ore-bearing fluids (COTTRANT, 1981; FLEET, 1983), the physico-chemical conditions of solute transport (BAU, 1991), the mechanisms of crystal growth (RAKOVAN and REEDER, 1996), or the dynamics of hydrothermal systems (MÖLLER and MORTEANI, 1983; MÖLLER et al., 1984). MÖLLER et al. (1976) investigated the systematics of the REE contents of fluorite, and found a correlation with the genetic type of the deposit: they were able to distinguish between fluorite of diagenetic, hydrothermal and magmatic origins.

Scheelite ( $\text{CaWO}_4$ ) is a mineral that, even if present in limited amounts, is widespread in a large variety of deposits (primary and placer) ranging in age from Early Archaean to Tertiary. Scheelite incorporates REE via the substitution of  $\text{Ca}^{2+}$  (up to 2.0 wt%  $\text{REE}_2\text{O}_3$ -total, SEMENOV, 1963). RAIMBAULT (1985) suggests a preferential uptake of HREE from a hydrothermal fluid by apatite, which leads to an enrichment about four times greater for Lu than for La, relative to the fluid. By comparing REE contents of cogenetic scheelite and apatite, RAIMBAULT et al. (1993) deduce that scheelite and apatite behave similarly during REE uptake from a fluid. Scheelite appears in the early assemblages of different types of mineralisations, and thus can record the REE patterns of early fluids. It is therefore a good monitor of the REE patterns of mineralising fluids. Additionally, scheelite shows a potential for Sm/Nd, Rb/Sr (ANGLIN, 1990; BELL et al., 1989; KENT et al., 1996) and Pb/Pb isotopic analyses.

We have used a newly developed type of luminescence spectroscopy, named thermal X-ray excited luminescence spectroscopy (XLT), to study 70 scheelites from deposits of various genetic type in the Alpine region. The luminescence spectra fingerprint the trace elements content of scheelite, and are particularly sensitive to some  $\text{REE}^{3+}$  ions substituting for  $\text{Ca}^{2+}$  in the scheelite crystal lattice. The main aim of this paper is to identify characteristic features or patterns among the luminescence spectra of scheelite, and then to correlate these features with geologically relevant parameters.

The knowledge of these regularities, combined with the flexibility of the XLT analytical method, forms the basis of a new approach to the study of different kinds of ore deposits. Some examples related to metallogeny and Au-prospecting will illustrate this method.

## Optical luminescence

REE optical luminescence resulting from different exciting radiations (e.g., X-rays, UV, electrons) has been recognised in many minerals including fluorite, apatite, carbonates, and scheelite (MARIANO and RING, 1975). For scheelite, two kinds of luminescence can be distinguished (inset in Fig. 1c):

(i) a broad peak of the so-called "self-luminescence" (SB = self-luminescence band) is an intrinsic property of the mineral, and has been attributed to a charge-transfer electronic transition in the molecular orbital scheme of the  $(\text{WO}_4)^{2-}$  (resp.  $(\text{MoO}_4)^{2-}$  in Mo-bearing scheelite) complex (GRASSER and SCHARMANN, 1976).

(ii) sharp peaks, called "characteristic peaks", are related to  $\text{REE}^{3+}$  ions in substitution of  $\text{Ca}^{2+}$ .

Therefore, in contrast to other analytical methods such as isotope dilution (ID), instrumental neutron activation (INA), or inductively coupled plasma mass spectroscopy (ICP-MS), luminescence spectroscopy discriminates between REE as structural admixtures in scheelite from REE present in foreign mineral inclusions within the scheelite matrix (e.g., monazite-(Ce) and xenotime-(Y), IVANOVA and POTY, 1992), in fluid inclusions, or absorbed on crystal surfaces. Quantitative evaluation of the spectra, though possible in certain cases (see e.g., COTTRANT, 1981 for scheelite), is not generally recommended due to practical problems, such as sample quantity, purity, and the presence of different admixtures that can quench (e.g.,  $\text{Fe}^{2+}$ ) or activate (e.g.,  $\text{Y}^{3+}$ , KEMPE et al., 1991) the luminescence of specific centres. The luminescence spectra, however, allow to characterise scheelite, and to qualitatively recognise some features of the trace element content of scheelite. Additionally, the luminescence technique is fast (2 min to obtain a spectrum), does not request sophisticated sample preparation (single raw grains up to 0.2 mm can be successfully analysed), and is relatively inexpensive. These qualities allowed us to build a reference database of more than 2000 luminescence spectra obtained using the techniques described below on scheelite from more than 300 localities world-wide.

## XL and XLT methods

### PRINCIPLES

X-ray excited luminescence (XL) spectra of scheelite usually display an intense and broad SB on which the characteristic peaks of REE are superposed (Fig. 1c). Many natural samples, such as

skarn scheelites (Fig. 1a), have elevated SB and/or decreased REE content and thus, the characteristic peaks are hidden by the SB.

During the last years, a new method for studying the REE-luminescence in natural scheelites was developed: the thermal X-ray excited luminescence (XLT; USPENSKY, 1994; USPENSKY and ALESHIN, 1993). LIMARENKO et al. (1978) studied the temperature dependence of SB and characteristic peaks of trivalent REE in synthetic scheelite crystals doped by Tb, and established that while the intensity of the SB quickly decreases with increasing temperature, the intensities of the characteristic REE peaks remain nearly constant. The XLT method takes advantage of this contrasted temperature dependence to obtain better characteristic peak/background values for all the peaks. An optimum temperature of 250 °C, low enough to avoid destabilisation of the REE<sup>3+</sup> luminescence centres, but high enough to achieve a significant decrease of the SB intensity, has been chosen on the basis of empirical tests. XL and XLT spectra for two samples are reported on figure 1. The XL spectrum (Fig. 1a) of the skarn scheelite with low REE content CHS3 displays

only the SB, whereas characteristic peaks (marked on all spectra by the symbols of the corresponding REE) are resolved on the XLT spectrum of the same sample (Fig. 1b). The SB disappears completely in the XLT spectrum of the sample from a molybdenite-aplite (SLT14: Figs 1c and 1d).

#### HOW TO READ THE XLT-SPECTRA

Table 1 shows the REE which can be studied using XL and XLT; for comparison, those REE which are quantifiable by ID are also listed. As discussed above, we will not try to extract quantitative data from the XLT spectra, but use them for comparison. Two XLT-spectra with corresponding chondrite normalised REE patterns are shown in figure 2. In all illustrated XLT-spectra, an asterisk near the sample number marks the spectra corresponding to samples for which a quantitative REE analysis is available.

To interpret the XLT spectra, the following points should be kept in mind:

(i) The Eu-anomaly ( $\text{Eu}^*/\text{Eu}$ ) describes the deviation of  $\text{Eu}_{\text{cn}}$  from a smooth chondrite nor-

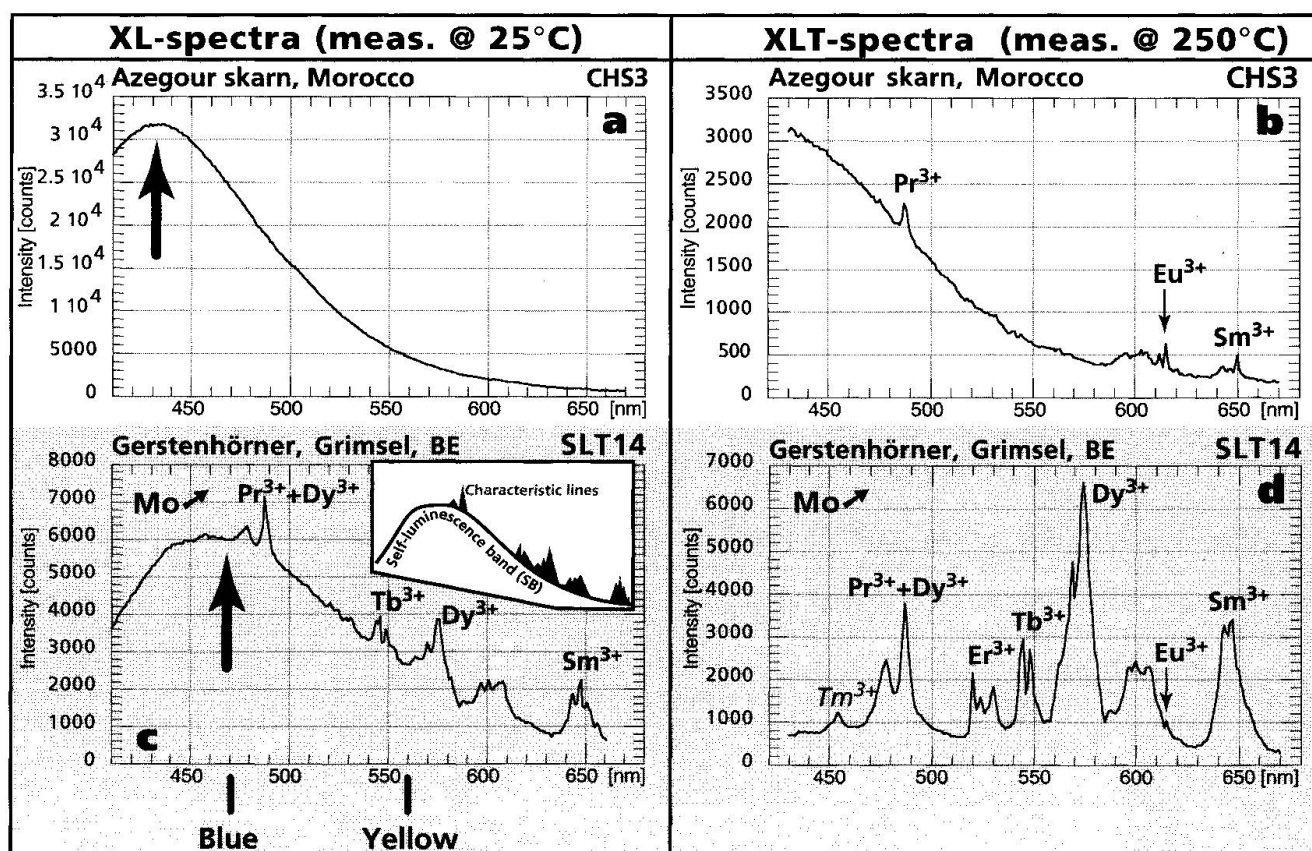


Fig. 1 Comparison of XL and XLT methods. The arrows on the XL spectra indicate the position of the SB maximum, which is shifted towards the yellow spectral area in the sample with elevated Mo-content (> 0.1 wt% Mo, Fig. 1c). The SB of pure powellite,  $\text{CaMoO}_4$ , occurs at 530 nm. In all the figures, the label "Mo↗" on a XLT spectrum indicates a scheelite with elevated Mo-content (i.e. more than about 0.1 wt%).



Tab. 1 REE determined by the XL/XLT (trivalent form) and ID methods.

	LREE (Light Rare Earths)							HREE (Heavy Rare Earths)							
	57 La	58 Ce	59 Pr	60 Nd	61 Pm	62 Sm	63 Eu	64 Gd	65 Tb	66 Dy	67 Ho	68 Er	69 Tm	70 Yb	71 Lu
XL			(X)	(X)		X	X	(X)	X	X	(X)	(X)	(X)	?	
XLT			X	(X)		X	X		X	X	(X)	X	(X)	?	
ID	X	X		X		X	X	X		X		X		X	X

Notes: Yb-luminescence (NIR-area of spectra) has not been observed in natural scheelites, but  $\text{Yb}^{3+}$  centers were discovered recently in natural scheelite crystals using low temperature electron spin resonance (HANUZA et al., 1994). The luminescence peaks of the elements in parentheses were not used in this study, though they may appear on some XL or XLT spectra: The Pr and Er peaks in the XL-spectra are mostly not usable for calculation. The characteristic Nd-peaks are located in the near infra-red (NIR) region (900–1100 nm), and their measurement requires special apparatus. Gd can only be measured by the XL method, because the intensity of this peak becomes unstable at higher temperatures. The luminescence associated to Ho is very weak even in the XLT-spectrum of the Ho-scheelite standard. Tm needs special attention because of complex overlap with some Dy-peaks.

malised plot, and is defined as  $\text{Eu}^*/\text{Eu} = 2 \text{Eu}_{\text{cn}}/(\text{Sm}_{\text{cn}} + \text{Gd}_{\text{cn}})$ , where the index (cn) refers to chondrite normalised values. A comparison of the XLT-spectra with the chondrite-normalised patterns produced in this study and available in the

literature shows that the ratio of the intensities of the  $\text{Eu}^{3+}$  and  $\text{Dy}^{3+}$  XLT-peaks can be used as an estimate of  $\text{Eu}^*/\text{Eu}$ :  $\text{Eu}^{3+}/\text{Dy}^{3+} > 2$  usually corresponds to scheelite with positive Eu-anomaly (e.g., Fig. 2 a, b), and  $\text{Eu}^{3+}/\text{Dy}^{3+} < 0.5$  to scheelite

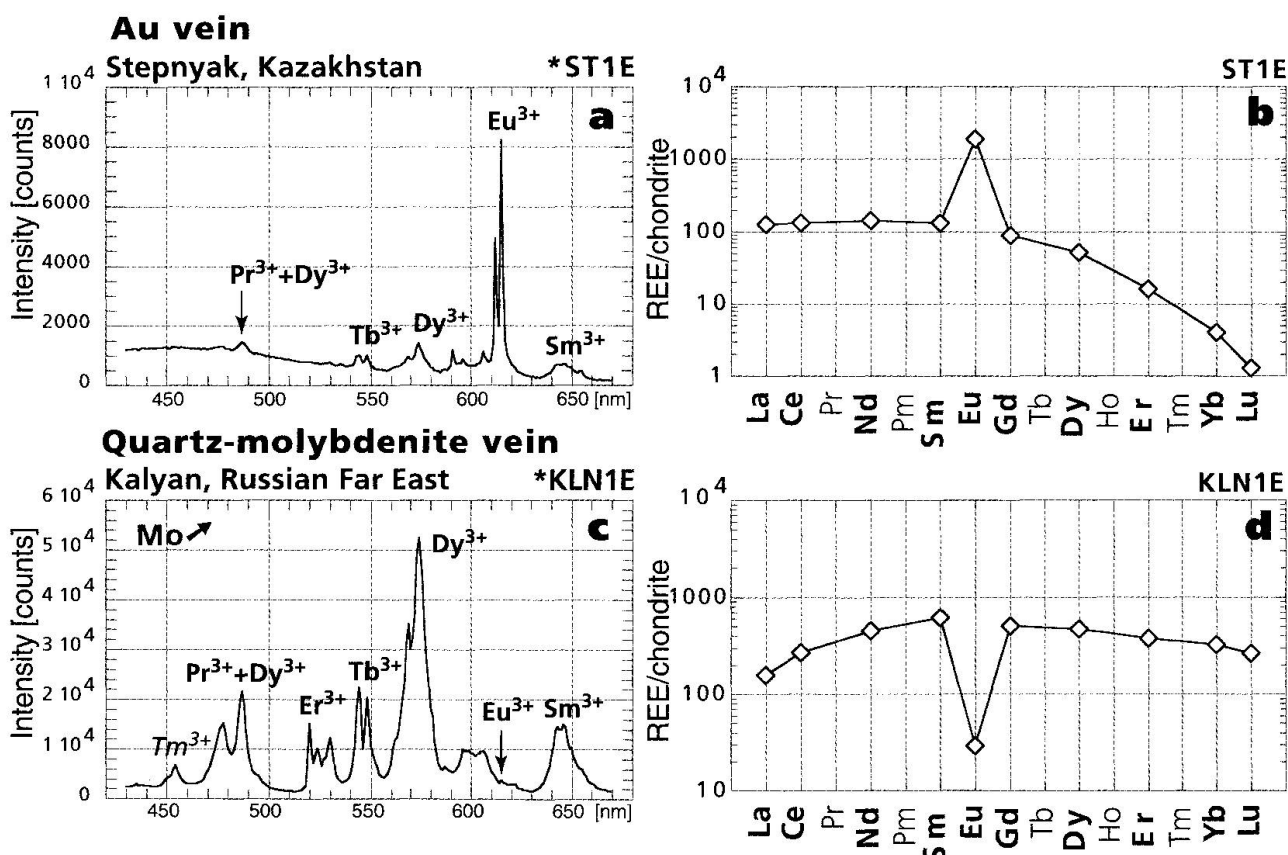


Fig. 2 Comparison of XLT spectra and chondrite-normalised REE data obtained by isotope dilution data. The Stepnyak Caledonian gold and scheelite-bearing quartz-carbonate-sulphide veins are situated inside a granodiorite stock and the intruded, altered volcanic-sedimentary rocks. The Mesozoic molybdenite-scheelite quartz veins ( $\pm$  fluorite, minor arsenopyrite and pyrrhotite) at Kalyan are situated in altered volcano-sedimentary rocks.

with negative Eu-anomaly (e.g., Fig. 2 c, d). One should keep in mind that scheelite can incorporate  $\text{Eu}^{2+}$ , which does not appear on XLT spectra. However, all the samples with high  $\text{Eu}^{2+}/\text{Eu}^{3+}$  ratios analysed to date had very high positive Eu-anomaly, and this was reflected in the  $\text{Eu}^{3+}/\text{Dy}^{3+}$  ratio (BRUGGER and USPENSKY, in prep.).

(ii) The  $\text{Sm}^{3+}$  and  $\text{Pr}^{3+}$  peaks, and in particular the  $\text{Sm}^{3+}/\text{Er}^{3+}$  ratio, are used to monitor the light REE (LREE).

(iii) The most important parameter for the classification of the XLT spectra is the ratio of the peaks  $\text{Er}^{3+}-\text{Tb}^{3+}-\text{Dy}^{3+}$ , which monitors the shape of a portion of the heavy REE (HREE) part of the pattern.

(iv) In some cases the relative enrichment of REE in scheelite can be inferred from the sum of the intensities of the characteristic peaks.

(v) The colour of the luminescence of scheelite under short wave UV allows to estimate the Mo-content of the mineral: blue: "Mo-free"; yellow:  $> 0.1\%$  Mo (TYSON et al., 1988; cf. column VLu in Tab. 2). The position of the SB maximum on the XL spectrum allows to refine this estimate (Fig. 1): it shifts from about 430 nm ( $< 0.05-0.1$  wt% Mo) to 475 nm ( $0.1-1.0$  wt% Mo) and to 480–530 nm (a few wt% Mo or more). The label [Mo] on the XLT spectra indicates scheelites with elevated Mo-content (i.e. more than about 0.1 wt% Mo, enough for changing the UV luminescence from blue to yellow).

## ANALYTICAL PROCEDURE

The XLT method was used to obtain the  $\text{REE}^{3+}$  luminescence spectra, and quantitative REE-analyses were carried out by ID on 11 scheelite samples to illustrate the chondrite normalised patterns associated to some common XLT-spectrum types, and to support the discussion of the luminescence data on Mt Chemin and Sotto Ceneri scheelites.

All scheelites were purified by hand picking under a binocular microscope coupled with a UV-lamp (Hg-bulb, 240 W and UFS5-filter with maximum of transparency near 260–300 nm). The concentrate was then crushed in a small agate mortar and sieved using copper mesh sieves. Each fraction was again examined for purity under the microscope. When sufficient scheelite was available, measurements were carried on the 0.15–0.25 mm fraction which was distributed over a surface of  $2 \times 4$  mm; in some cases, however, several individual scheelite grains (0.05–0.1 mm in size), or even single grains (about 0.2–0.5 mm) have been used. Test measurements have shown good agree-

ment between the XLT-spectra obtained on a typical preparation and a single grain from the same scheelite sample.

X-rays (30 kV, 60  $\mu\text{A}$ ) from a small medical X-ray tube, which produces wide-angle radiation, pass through a thin aluminium plate on which the sample is located. XLT spectra were collected at 250 °C in air, in the 400–700 nm spectral area.

The experimental equipment consists of a MDR23-monochromator (LOMO, St Petersburg, Russia) coupled with a FEU100 photomultiplier (200–800 nm). The operating software was written by Gregory L. Stesik, and that for spectra processing by Alexey P. Alioshin (IGEM Russian Academy of Sciences). The latter program calculates the intensities of characteristic peaks corrected for influences from SB and spectral interferences, and yields the following tables, which can be requested from the senior author: (i) intensities; (ii) intensities normalised to the most intense peak in the spectra; (iii) different ratios of characteristic peaks.

The following characteristic peaks were selected by considering the XLT spectra obtained on synthetic scheelites doped with individual  $\text{REE}^{3+}$  (1000–3000 ppm):  $\text{Tm}^{3+}$  – 453 nm;  $\text{Pr}^{3+}$  – 487 nm;  $\text{Er}^{3+}$  – 520 nm;  $\text{Tb}^{3+}$  – 544 nm;  $\text{Dy}^{3+}$  – 574;  $\text{Eu}^{3+}$  – 615 nm;  $\text{Sm}^{3+}$  – 643 nm. Synthetic scheelites were created by keeping stoichiometric mixtures of  $\text{Na}_2\text{WO}_4 \cdot 2\text{H}_2\text{O}$  and  $\text{CaCl}_2 \cdot 2\text{H}_2\text{O}$ , together with the REE chloride of interest, for 2 hours at 900 °C in open quartz tubes filled with molten NaCl, and then slowly cooling them to room temperature during 20 hours. After washing with distilled water, we obtained colourless crystals of scheelite, 0.01–0.5 mm in size. These scheelites exhibit luminescence spectra similar to those of CARUBA et al. (1983).

Because the main  $\text{Pr}^{3+}$  peak coincides with a  $\text{Dy}^{3+}$  peak (in the figures, the  $\text{Pr}^{3+}$  peak is usually labelled as " $\text{Pr}^{3+} + \text{Dy}^{3+}$ "), we used the formulae (1), resp. (2) for scheelite in which  $\text{Dy}^{3+}$  is absent, to calculate the "real" value of the  $\text{Pr}^{3+}$  peak (meas = intensity measured on the sample; synth = intensity measured on the synthetic scheelite containing only Dy; corr = intensity corrected for the interference; the position of the peak is given as an index):

$$(1) \left\{ \begin{array}{l} \text{corr}_{487\text{nm}} \text{Pr}^{3+} = \text{meas}_{487\text{nm}} \text{Pr}^{3+} - k_1 \frac{\text{meas}_{478\text{nm}} \text{Dy}^{3+}}{\text{synth}_{478\text{nm}} \text{Dy}^{3+}}; \quad k_1 = \frac{\text{synth}_{487\text{nm}} \text{Dy}^{3+}}{\text{synth}_{478\text{nm}} \text{Dy}^{3+}} = 1.14 \\ \text{corr}_{574\text{nm}} \text{Pr}^{3+} = \text{meas}_{574\text{nm}} \text{Pr}^{3+} - \frac{\text{meas}_{574\text{nm}} \text{Dy}^{3+}}{k_2}; \quad k_2 = \frac{\text{synth}_{574\text{nm}} \text{Dy}^{3+}}{\text{synth}_{487\text{nm}} \text{Dy}^{3+}} = 4.12 \end{array} \right.$$

## Sample description and scheelite metallogeny

The list of scheelites from the Alps which were studied by the XLT method is given in table 2, and

Tab. 2 Samples analysed by the XLT method for this study.

SLT	so	Number	XLT type	Locality, valley, canton/country	Tectonic unit	Comments	VLu	Col
1	MBE	BEA7574	Tb	near "Goldene Sonne" mine, Calanda, GR	Helvetic	Euhedral crystal in vug	b/lw	y
2		CHS2 vein	Tb	near "Goldene Sonne" mine, Calanda, GR	Helvetic	Massive in a quartz vein	b	l br-y
3		CHS2 vug	Tb	near "Goldene Sonne" mine, Calanda, GR	Helvetic	Euhedral crystal in vug	b	l br-y
4		SCH 120	Tb	near "Goldene Sonne" mine, Calanda, GR	Helvetic	Massive in a quartz vein	b	l br-y
5	MGL	MGL63042	St	Burstspitze, Lötschental, VS	Aar-massif	Rock forming mineral	b	w
6,7,8	IFR	UF 143, 144, 145	St	Burstspitze, Lötschental, VS	Aar-massif	Rock forming mineral	b	w
9	MGL	UF152	St->Au	Burstspitze, Lötschental, VS	Aar-massif	Rock forming mineral	b	w
10	MBS	P3434	Tb	Tunnel Mittal-Hohtenn, Lötschental, VS	Aar-massif	Euhedral crystal in vug	b/lw	br
11	We	Ba1	Ap	Alpajhorn, Baltschiederthal, VS	Aar-massif	Grains within quartz-molybdenite vein	b	w
12	We	Ba1.1	Ap	Alpajhorn, Baltschiederthal, VS	Aar-massif	Altered vein	b	w
13	MGL	MGL63045	Ap	Alpajhorn, Baltschiederthal, VS	Aar-massif	Grains in vein	b	w
14	MBE	BEA8281	Mo	Gerstenhömer, Grimsel, BE	Aar-massif	Grains in vein	y	w-y
15	MGL	MGL58902	Mo	Nägelisratli, Grimsel, BE	Aar Massif	Grains in quartz with molybdenite	y	w
16	MBE	BEB8635	Mo	Deponie Wasserschloss Kessiturm, Grimsel, BE	Aar-massif	Grains in vein	y	w
17	MBE	BEB2934	SB	Unwäzwerk Grimsel-Oberaar, BE	Aar-massif	Good crystal in vug (Found 1887)	w-b	t
18	MBE	BEB7592	SB	Kammegg near Guttannen, Haslital, BE	Aar-massif	Good crystal in vug (Found 1918)	w-b	t
19	We	SMCr2091	Mo	Freisiegelstollen Sta Maria-Cristallina, GR	Gotthard	Grain in a shearzone with chalcopyrite	w	w
20	MBE	BEB5727	SB	Alpe di Boverina, Val di Campo, TI	Gotthard	Euhedral crystal in vug	b/lw	gr-g
21		CHS1	St->Hy	Robert mine, Salanfè, VS	Aig. Rouges	Skarn mineral	b	w
22	MGL	MGL58062	St	La Creusa, Trient Valley, VS	Aig. Rouges	Rock-forming mineral	b	w
23	MGL	MGL63040	St	La Creusa, Trient Valley, VS	Aig. Rouges	Rock-forming mineral	b	w
24	MGL	MGL58061	Au+SB	Luisin, Trient valley, VS	Aig. Rouges	Rock-forming mineral	b	y-br
25	MGL	MGL63039	Tb	Fluorite mine, Tête des Econduits, VS	Mont Blanc	Dissemination in a (metamorphically recrystallised) quartz-fluorite vein	bw	
26		SWZ86	Tb	Fluorite mine, Tête des Econduits, VS	Mont Blanc	Thin (0.1-0.5 mm) fracture in host rock of the quartz-fluorite vein		
27, 28, 29		CHS4, SWZ75, SWZ79	Tb	Tête des Econduits, Mt Chemin, VS	Mont Blanc	Euhedral crystal in vug	b	l-br
30	MGL	MGL63046	Tb	Road tunnel, Mt Chemin, VS	Mont Blanc	Euhedral crystal in vug	b	t
31	MGL	SCH113	Tb	Near "Chez Larze" Quarry, Mt Chemin, VS	Mont Blanc	Massive in a quartz-siderite vein	b?	w
32		SWZ76	St->SB	Couloir Collaud, Mt Chemin, VS	Mont Blanc	Gram in a discordant quartz, epidote, stilpnomelane veinlet in a Fe-skarn		
33	MGL	MGL63037	St	Liez river near St Martin, Hérens valley, VS	Siviez-Misch.	Remobilisation in quartz-exsudate	b	w
34	MGL	MGL63043	St	Mission river, Val d'Anniviers, VS	Siviez-Misch.	Rock-forming mineral	b	w
35	CA	SCH114	Au	Filone Quarazzolo, Val Quarazzo, NO, Italy	Mont Rose	Massive scheelite in quartz vein	b	y-br
36	FV	SCH101	(Ma)	Campria, Val Vigizzo, Italy	Southern Alps	Crystals in quartz-rich pegmatitic vein	b/lw	br
37	MBS	M23504	Tb	Iragna, Leventina, TI	Leventina	Euhedral crystal in vug	b	w-y
38	MBE	M28315	Tb	Cava Bugheroni near Iragna, Leventina, TI	Leventina	Euhedral crystal in vug	b	lwy
39	MGL	SCH106	Tb	Quarry west of Blon, near Iragna, Leventina, TI	Leventina	Euhedral crystal in a vug within a quartz vein	b	l-y
40	MGL	SCH107	Tb	Quarry "Lodrino" N-W of Dundro near Iragna, Leventina, TI	Leventina	Euhedral crystal in vug	b	l-y
41	HR	SWZ74	Hy+Mo+SB	Mendel river near Disentis, GR	Tavetsch	Heavy mineral concentrate (river)		
42	MGL	MGL37596	Mo	Traversella Mine, Aosta valley, Italy	Austroalpine	Euhedral crystal in magnetite ore	y	w

SLT	so	Number	XLT type	Locality, valley, canton/country	Tectonic unit	Comments	VLu	Col
43	MGL	SCH108	Hy+SB	Miniera di Brosso, TO, Italy	Austroalpine	Euhedral crystal in vug	b/lw	br-t
44	We	V22	St	Val Scareglia, Val Colla, TI	Southern Alps	Discordant veinlet	b	l-y
45	We	CHS5	St->Au	Val Firinescio, Sotto Ceneri, TI	Southern Alps	Discordant veinlet	b	w-y
46	We	CHS6	Hy	Sotto Ceneri, TI	Southern Alps		b	w-y
47	We	CW3	St	Sotto Ceneri, TI	Southern Alps	Discordant quartz-scheelite vein	b	l-y
48	We	CW33	Hy	Sotto Ceneri, TI	Southern Alps	Centimetre-large scheelite aggregates in discordant veinlet	b	w
49	We	CW71	Au	Val Pirocca, Sotto Ceneri, TI	Southern Alps	Discordant chlorite vein; scheelite occurs as a 4x3 cm masse	b/lw	y-br
50	We	CW32	St->Hy	Sotto Ceneri, TI	Southern Alps	Rare aggregates (< 1 mm) within rock, in a layer subparallel to schistosity	b	l-y
51	We	CW1	CS->Hy	Sotto Ceneri, TI	Southern Alps	Aggregates (1 cm) in the rock	b	l-y
52	We	CW166	Hy	Sotto Ceneri, TI	Southern Alps	Aggregates (1 cm) in the rock	b	w
53	We	CW170	CS->Hy	Sotto Ceneri, TI	Southern Alps	Aggregates (1 mm) within the rock	b	l-y
54	RZ	Z192	CS	South of Monte Giove, NO, Italy	Southern Alps	In a calcisilicate xenolith within "Cenerigneiss"	b	w
55	MGL	SCH111	SB	Quarry of Claro, Bellinzona, TI	Lucomagno	Thin "films" around calcite grains	b	w
56	MGL	MGL63038	Ap	Albignaglescher, Engadine, GR	Bergel intr.	Large grains in a smoky quartz vein	w-y	l-y-w
57	MBE	BEB6265	Ap	Val Forno, Engadine, GR	Bergel intr.	Grains in vein	b	w
58	MGL	SCH102	St->Hy	Val de Nendaz, VS	Siviez-Misch.	Heavy mineral concentrate (river)	b	w
59	MBE	M6006	SB	Rotlaur near Guttannen, Haslital, BE	Aar-massif	Well-shaped crystal in vug	b	t
60	MGL	MGL63044	St	Tännbach over Ergisch, Turtmanntal, VS	Siviez-Misch.	Rock-forming mineral	b	w
61	MGL	SCH100	St	Gollyre mine, Ayer, Val d'Anniviers, VS	Siviez-Misch.	Heavy mineral concentrate (amphibolite-bearing scree)	b	w
62	CA	SCH103	Hy	Val Toppa, Filone della Piana, NO, Italy	Austroalpine	In small vugs	b	l-y
63	MGL	SCH109	Au	Val Toppa, Filone della Piana, NO, Italy	Austroalpine	Massive, in a quartz-siderite veinlet	b	ly
64	CA	SCH117	Hy	Formasco Au vein, Pieve Vergonte, Italy	Austroalpine	Massive scheelite with strolzite	b	w
65	CA	SCH116	Hy	Mte Gorio, Baceno, Italy	Antigorio	Euhedral crystal in vug	b	y
66	CA	SCH118	Ma	Baveno, Italy	Southern Alps	Good crystal in pegmatite pocket	b	l-br
67	MGL	TV06	Mo	Precise location unstated	Mont Rose	Rock forming mineral	b	w
68	MGL	SCH105	Ma	Alta Valle Cervo, Biello, Italy	Southern Alps	Masses in thin vugs	y	w
69	MGL	SCH119	Ma	Haut Poirot, Gerardmer, Alsace, France	Vosges Basement	Masses up to 1 cm in Mn ore	y	w
70	MGL	MGL63041	St	Mittersill, Austria	Austroalpine		b/l-y	w
71	WP	AUS4	Au	Schellgaden deposit, Austria	Murek nappe (Penninikum)	With quartz	b	l-y
72	WP	AUS7	Au	Silberpfennig deposit, Austria	Central Gneiss (Penninikum)	With quartz	b	l-y
73	WP	AUS9	Mo	Bedovina deposit, Italy		With chalcocopyrite and quartz	y	w

**Column SLT:** sample number used in this paper; the localisation of most samples is given on the map of figure 3; **column so:** source of the samples; IFR = collection UROMINE at the Institute for Mineralogy and Petrography, Fribourg; MBE, MBS, MGL = Natural History Museums of the cantons Bern, Basel, and Vaud, respectively; We = collection of WENGER (1987) at the Institute for Mineralogy and Petrography, Bern. Private collections: CA-C. Albertini, FV-F. Vanini, HR-H. R. Rück, RZ-R. Zurbruggen, WP-W. Paar; **column number:** original sample number in the source collection; **column XLT type:** classification of the XLT spectrum according to the groups defined in this study; CS = Skarn and calcisilicates; Mo = Molybdenite-vein; Ap = Molybdenite-vein, type Alpihorn; Ma = acid to intermediate magmatic rocks; St = Stratabound metamorphic; Hy = Hydrothermal; Tb = hydrothermal, Tb-subtype; Au = hydrothermal, Au-subtype; SB = hydrothermal, elevated SB subtype; **column VLu** = colour of visual luminescence; **column Col** = colour of sample; prefix l = light, b = blue, br = brown, t = colourless/transparent, g = green, gr = grey, w = white, y = yellow.

Abbreviations for the Swiss cantons: BE-Bern, GR-Graubünden, TI-Ticino, VS-Valais.



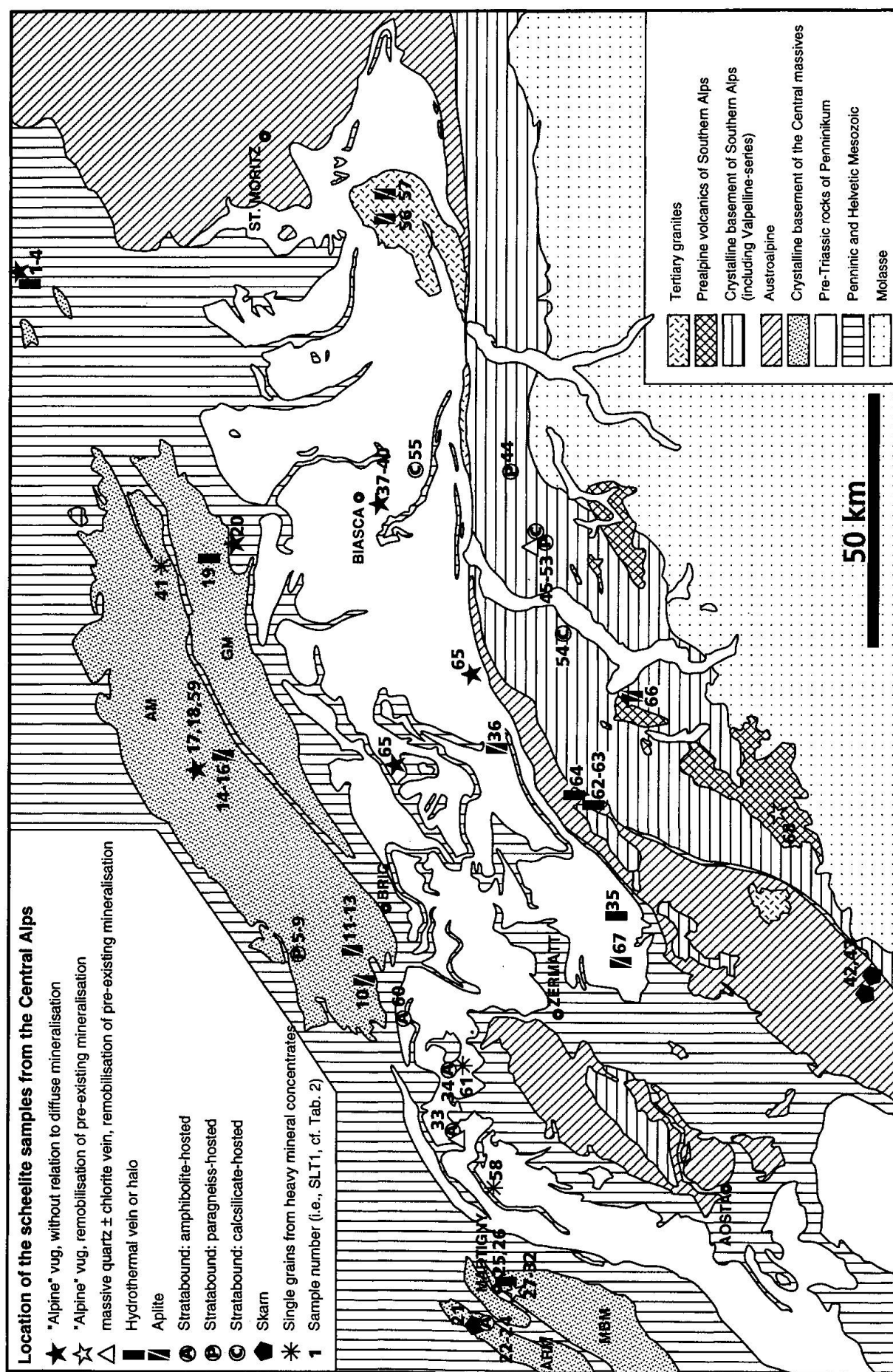


Fig. 3 Simplified tectonic map of the Alps (modified after WENGER, 1987). Location and deposit type of the samples are plotted. AM = Aar Massif, GM = Gotthard Massif, MBM = Mt. Blanc Massif.



the location of the samples from the Central Alps is indicated on figure 3. The variety of geological settings encountered in the Alps allows sampling of scheelite of various ages and genetic types. This section presents a brief geological and metallogenic overview of the mineralisations from which the samples were collected. Emphasis is given to the parameters that could be correlated with the characteristics observed in the XLT-spectra; some of the scheelite occurrences which are not well known are discussed in greater detail.

This section also may be read as an introduction to the metallogeny of scheelite, and illustrates the very large variety of deposits in which this mineral appears.

### SKARN

The formation of Au-rich arsenopyrite-bearing skarn at Salanfe (VS) is related to a leucogranite, which formed by partial melting of Ordovician (?) granitoids during a Variscan regional metamorphic event. After an initial "metamorphic stage", the skarn shows a typical evolution from prograde (stability of H<sub>2</sub>O-free minerals such as hedenbergite) to retrograde stage (pyroxene altered to chlorite, amphibole and epidote; CHIARADIA, 1993). The main scheelite generation is deposited in the early prograde stage in association with pyroxene and allanite (CHIARADIA, 1993), and a second generation (not studied here) appears at the end of the retrograde stage. The precipitation of Au-bearing arsenopyrite begins during the prograde stage but post-dates the main scheelite generation, and continues during the retrograde stage. CHIARADIA (1994) infers a sedimentary enrichment of W in metagraywacke (Upper Proterozoic to Cambrian) possibly by exhalative processes, and suggests that the W deposited in the skarn was extracted from the metagraywacke and not from the anatexic leucogranite, the latter acting just as a motor for hydrothermal convection.

Euhedral scheelite crystals up to more than 1 cm in size occur in the Fe-B-skarns of Brosso and Traversella (Italy). Both skarns are situated in the metamorphic formations of the Sesia Lanzo zone (micaschists with eclogite and dolomitic marble intercalations) at the contact with the Tertiary Traversella pluton (monzodiorite to granodiorite). A complex evolution from skarn to hydrothermal quartz-arsenopyrite veins is observed (GIUSSANI, 1978).

### MOLYBDENITE-APLITES AND MOLYBDENITE-BEARING QUARTZ VEINS

Many molybdenite-aplites occur in the Aar massif, some of them containing scheelite (e.g., Gerstenhörner, Nägelisrali; STALDER and WENGER, 1988). A stockwerk of such aplites in a Pre-Variscan orthogneiss (granodiorite) at the contact between the Hercynian Central Aar granite and the old basement at Alpjahorn in Baltschiedertal represents the largest Swiss Mo-deposit (ENGEL et al., 1986).

Within the Tertiary Bergell granite, scheelite is reported from smoky quartz veins ( $\pm$  Bi-sulfosalts, molybdenite, ...; MAURIZIO and MEISSER, 1993; PARKER, 1973). At Bedovina (Predazzo, Italy), a stockwerk of veins with scheelite, chalcopyrite,  $\pm$  pyrite,  $\pm$  stibnite,  $\pm$  molybdenite and  $\pm$  monazite crosscuts a Triassic monzonite (ZUFFARDI, 1989).

### ACID TO INTERMEDIATE MAGMATIC ROCKS; PEGMATITES

Many plutonic rocks bear small amounts of scheelite. Thin vugs in the monzonite in Valle Cervo (Italy) and the pegmatitic pockets of the Permian Baveno granite contain this mineral. Scheelite together with chalcopyrite occurs in a shear zone within the Cristallina meta-granodiorite (Gotthard Massif; WENGER, 1987). The Mn-(Ba, W) vein of Haut Poirot, in the Variscan two-micas Remiremont granite, represents a typical intra-granite mineralisation (FLUCK and WEIL, 1975).

### STRATABOUND METAMORPHIC DEPOSITS

In this important group of deposits, W-enrichment in volcano-sedimentary rocks pre-date metamorphism during which scheelite re-crystallised. The large Felbertal deposit (Austria) belongs to that group, but is not discussed here.

### Canton of Valais (Switzerland; Penninic domain and External massifs)

Many, mostly small-sized stratabound deposits have been found during the UROMINE prospecting project (WOODTLI et al., 1987) in the basement of the Aar massif (Burstspitze, Lötschental) and in the Pre-Westphalian basement of the Siviez-Mischabel nappe (Val d'Hérens, Val d'Anniviers, and Turtmanntal). These deposits are related to inhomogenous, am-

phibolite-bearing series, whereby the mineralisation predates a Variscan, amphibolite-facies metamorphism. At Burstspitze, W is associated with a Bi-Ag  $\pm$  Pb anomaly. Scheelite has also been found in the amphibolites of the Aiguilles Rouges massif (Luisin, La Creusa). An early (syn-genetic to diagenetic) enrichment of W is assumed for all these stratabound deposits (WOODTLI et al., 1987).

#### **Sotto Ceneri (Switzerland and Italy)**

The Sotto Ceneri belongs to the crystalline basement of the Southern Alps, which underwent a complex polyphase evolution: the Caledonian metamorphism produced migmatitisation and led to intrusion of the protolith of the "Cenerigneiss" into metasedimentary sequences. After exhumation, sedimentation took place on these metamorphic rocks (e.g., clayish sandy schists of Val Colla). The Hercynian metamorphism occurred under upper greenschist to amphibolite facies conditions, and, during Permian, this basement was penetrated by numerous dykes. Many vein deposits (Fe-As-Au; Sb-Au) occur in Sotto Ceneri (mostly in the Malcantone). Their formation post-dates the dykes intrusion, but still seems to be related to the Permian volcanism (KÖPPEL, 1966).

Several types of scheelite mineralisation can be distinguished: *in the "Ceneri-zone"*: (1) in calc-silicate bed; (2) in biotite-gneiss ("Cenerigneiss"), (2a) along schistosity, (2b) in discordant quartz-chlorite veinlets; *in the clayish-sandy schists of Val Colla*: (3a) within concordant calc-silicate-bearing, quartz-rich layers; (3b) in discordant shear zones and quartz veinlets (WENGER, 1983, 1987).

WENGER (1987) proposed an early (sedimentary exhalative to epithermal) input of W in the "Cenerizone". This mineralisation has been re-worked several time (Caledonian and Hercynian metamorphisms, Permian volcanism). The clayish-sandy schist of Val Colla is the product of the erosion of rocks which already contained a W mineralisation. The main mineralisation within the Val Colla schist seems to be related to hydrothermal activity connected to the acid Ordovician volcanism (WENGER, 1987; ZURBRIGGEN, 1996).

### **HYDROTHERMAL DEPOSITS**

#### **"Alpine vugs"**

In this paper, we will use the expression "Alpine vug" to describe open fractures occurring in

quartz ( $\pm$  carbonate) veins related to the Alpine metamorphic evolution. In some cases, scheelite from an "Alpine vug" is directly related to a stratabound/vein W-mineralisation. However, many isolated Alpine vugs contain scheelite but are not related to any recognised W-mineralisation. The famous mega-crystals from Kammegg, Haslital, BE (a crystal of 932 g found in 1887 was the largest scheelite crystal known in Europe at that time; STALDER and WENGER, 1988; PARKER, 1973) come from a vug containing quartz, adularia, actinolite-asbestos, epidote, chlorite, and goethite within an amphibolite of the Aar-massif basement. Intensive prospecting with UV lamps, however, could not locate any disseminated W-mineralisation (STALDER, oral comm.). Another similar find is reported from Alpe di Boverina (Val di Campo, TI) in "Alpine vugs" with quartz  $\pm$  scapolite, pyrite, rutile, muscovite, tourmaline inside the Triassic "Quartenschiefer" belonging to the Mesozoic "Muldenzone" of the Gotthardmassiv (TORONI, 1984). Scheelite crystals up to 3 mm in diameter occur in "Alpine vugs" from the Leventina gneiss near Iragna and Lodrino, TI (BIANCONI and SIMONETTI, 1967), and were formed as a result of remobilisation from Ti-Mo-W-U-pegmatites. The scheelite crystals from the Tunnel Mittal-Hohtenn (Lötschental, VS) represent Alpine mobilisation of W from a Mo-aplite within the Aar-Massif basement (GRAESER, 1984).

#### **Au-deposits**

A stockwerk of quartz-carbonate-fluorite-gold-pyrite-arsenopyrite-scheelite veins associated with extensive hydrothermal alteration occurs in the core of an Anticline in Mesozoic sediments of the Helvetic domain near Felsberg ("Calanda" deposit, GR). Scheelite up to 1 cm in size appears as xenomorph grains in quartz, and as euhedral crystals in numerous vugs (grown on quartz and fluorite crystals) or in fluorite masses; disseminated scheelite occurs mostly within Dogger carbonate-bearing sandstones (graphite and hematite locally abundant; BÄCHTIGER, 1974; BÄCHTIGER et al., 1972). According to AUDÉTAT (1995) the burial of the "Tavetscher Zwischenmassiv" underneath deeper crustal layers released huge quantities of fluids which have been concentrated along the axial plane of an anticline. During the latest stage of the fluid-rock interaction, Au was precipitated by boiling. The whole mineralising event took place between 210–350 °C, and 1–3 kbar.

In the Val Toppa (Italy), several quartz-sulphide  $\pm$  gold-scheelite veins crosscut the main

schistosity of the "Scisti cristallini della zona del Canavese", a < 5 km thick band between "zona diorito-kinzigita principale" to the SE and "seconda zona dioritica" to the NW, at the Eastern limit of the "Sesia-Lanzo" zone (STELLA, 1943).

The "Filone Quarazzola" in Val Quarazzo (Provincia di Torino, Italy) is a quartz  $\pm$  pyrite-arsenopyrite-scheelite-gold vein occurring in the "gneiss ghiandone" in the Monte Rosa nappe (STELLA, 1943).

The Schellgaden (Austria) stratabound W, Au, Pb, Zn, (Mo), Te, (As), B and F deposit is hosted by schists and quartzite lenses belonging to the Murek nappe (Penninic zone of Eastern Hohe Tauern), which mostly consists of amphibolites, hornblende gneisses and migmatites. An origin contemporaneous with the host rock, possibly by exhalative processes, seems likely for this deposit (FINLOW-BATES and TISCHLER, 1983).

The Silberpfennig (Austria) quartz-sulphide  $\pm$  scheelite vein deposit is hosted by the "Central Gneisses" of the Penninic zone of Eastern Tauern, and it belongs to the Siglitz province (EXEL, 1993).

The Disentis (GR) Au-anomalies are embedded in chert layers within fine-grained sericite and sericite-muscovite schists, whose protolith could be tuffs containing some ultrabasic rocks. These series belong to the Tavetsch Crystalline Massif, which separates the Gotthard Massif from the Aar Massif (KNOPF et al., 1989). Three main stratabound Au-mineralisations have been recognised; they are associated with wide hydrothermal alteration haloes characterised by sericitisation and carbonatisation. Two types of mineralisation can be distinguished: (i) massive sulphide beds (up to 5 cm and 8.5 g/t Au) and (ii) disseminated sulphides in quartz-rich rocks; ore minerals are pyrite, arsenopyrite, pyrrhotite, magnetite,  $\pm$  stibnite,  $\pm$  bismuthinite,  $\pm$  sphalerite,  $\pm$  galena,  $\pm$  ilmenite,  $\pm$  tetrahedrite,  $\pm$  chalcopyrite. Gold crystals sometimes occur in "Alpine vugs" together with quartz crystals. Scheelite up to now has not been described from the lode ore, but it occurs together with Au in the heavy concentrates of the Medel river near Disentis.

#### The occurrences from Mt Chemin

The Mt Chemin near Martigny (VS) represents the NE end of the Mt Blanc Massif. A paragneiss series with amphibolite and marble intercalations was subjected to a Variscan amphibolite facies metamorphism, and was intruded by the late Variscan Mt Blanc granite (304 Ma, BUSSY, 1990); marbles were locally transformed into andradite-magnetite skarn. Some fluorite-quartz ( $\pm$  barite,

galena, sphalerite) veins were emplaced in the basement after the crystallisation of the Mt Blanc granite, but before the deposition of Triassic sediments (WUTZLER, 1983). During the Alpine orogeny, all these rocks and deposits underwent metamorphism at greenschist facies conditions.

The main scheelite mineralisation at Mt Chemin occurs at the "Tête des Econduits" and is located in a quartz-porphphyry dike related to the Mt Blanc granite. Veinlets of massive scheelite up to 5 cm in thickness crosscut the rock. Most of the scheelite has been redeposited in a network of Alpine quartz veins, which display many vugs in which scheelite crystals coexist with quartz, adularia, pyrite, fluorite and various, relatively abundant REE-minerals. An associated Au-mineralisation, where native gold occurs in altered pyrite, has been recognised recently. A maximum age of 12 Ma ( $^{40}\text{Ar}/^{39}\text{Ar}$  adularia) and temperatures of 250–350 °C are reported for this mineralisation (MARSHALL, 1995). Furthermore, scheelite has been reported in very small quantity from four other localities at Mt Chemin: (i) near Chez Larze, an "Alpine vein" bears quartz, siderite, and scheelite [SLT31]; (ii) one sample of a quartz-calcite-pyrrhotite vein collected on the dumps of the Road Tunnel "Mt Chemin" (17.9.89) contains one scheelite grain, 1 cm in size [SLT30]; (iii) in the fluorite mine, scheelite grains smaller than 1 mm occasionally occur within the massive fluorite, or in thin fractures (0.1–0.5 mm thick) in the embedding rocks [SLT25,26]; (iv) quartz-epidote-amphibole veinlets crosscutting the Fe-skarn in Couloir Collaud occasionally bear scheelite; MARSHALL, (1995) gives PT values from 365 °C at 2.5 kb to 425 °C at 5.2 kb along a fluid inclusion isochore for that vein type [SLT32].

It should be noted that mobility of REE at Mt Chemin during Alpine metamorphism is documented by the occurrence of REE minerals in different types of "Alpine vugs" (MEISSER and ANSERMET, 1993).

#### Global features among the XLT Spectra of scheelite from the Alps

Some chondrite normalised REE patterns can be found on figure 4 (data on Tab. 3). The bivariate plot of figure 5 uses the  $\text{Eu}^{3+}/\text{Dy}^{3+}$  peaks ratio from the XLT spectrum as an estimate of the Eu anomaly, and  $\text{Er}^{3+}/\text{Tb}^{3+}$  as a marker of the shape of the REE pattern. This simple variation diagram allows to discriminate between scheelite formed within different genetic types of ore deposits. Consideration of the whole XLT-spectra allows a finer discrimination among the groups presented

Tab. 3 ID REE data (ppm) in scheelites from the Alps and from two reference deposits.

Sample	Locality	La	Ce	Nd	Sm	Eu	Gd	Dy	Er	Yb	Lu
SLT3	Calanda (GR)	29.01	209	368.4	145	27.1	140	101	30.1	8.03	0.69
SLT14	Gerstenhörner (BE)	100.6	508.1	756.5	371	3.12	389	397	181	132	18.1
SLT21	Salanfe (VS)	3.706	20.59	46.26	28.7	10.3	43.9	55.9	27.3	12	0.91
SLT27	Tête des Ecouits, Mt Chemin (VS)	25.52	275	621	536	44.2	545	456	142	76.1	7.0
SLT33	Liez River (VS)	0.076	0.297	0.583	0.47	0.25	1.36	4.39	9.3	28.7	6.56
SLT30	Road tunnel, Mt Chemin (VS)	0.781	5.342	16.06	14.9	4.9	38.3	48.2	17.6	4.55	0.45
SLT35	Filone Quarazzolo (Italy)	101	401.5	256	66.8	125	59.3	52	16.9	6.88	0.54
SLT45	Val Finesco (TI)	17.54	50.37	26.23	5.19	18.2	5.49	6.11	6.57	9.48	2.53
SLT49	Val Pirocca (TI)	2.731	11.33	12.92	4.01	21.7	4.51	4.72	3.83	6.15	1.35
ST1E	Stepnyak (KZ)	41.25	111.6	88.03	26.5	143	24.6	17.3	3.6	0.88	0.04
KLN1E	Kalyan (RFE)	51.21	232.5	283.8	125	2.23	139	159	83.6	70.6	8.79

Notes: KZ = Kazakhstan; RFE = Russian Far East.

in figure 5, as well as the definition of some other groups.

The principal characteristics of each recognised group are summarised in table 4, whereas

typical spectra may be found in figures 6 and 7. Our large worldwide database of > 2000 spectra shows that these features described below are of global significance. In the following, the charac-

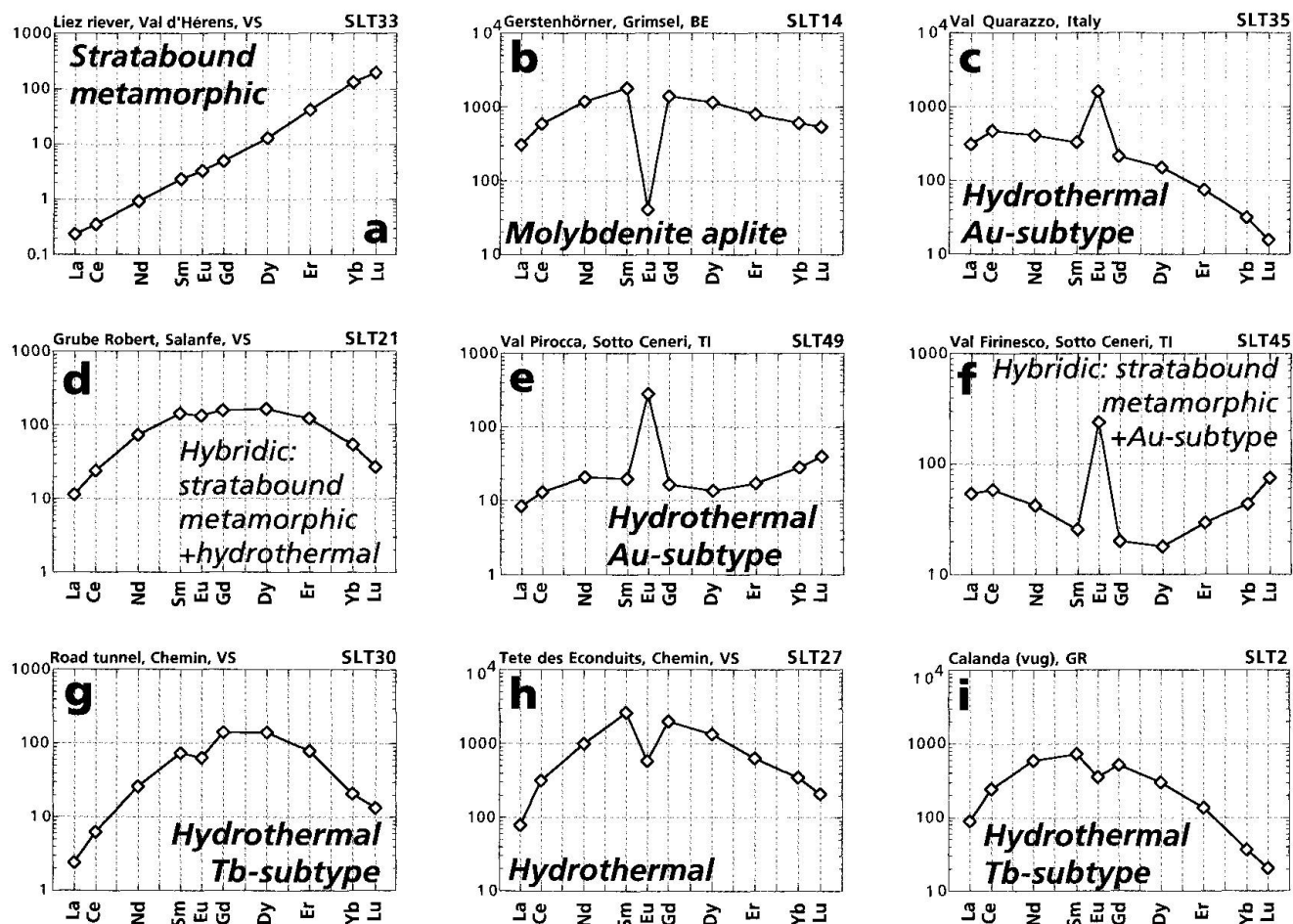


Fig. 4 Chondrite-normalised (after EVENSEN et al., 1978) REE data (by isotope dilution) for scheelites from the Alps (Data in Tab. 3). The type of the scheelite according to its XLT-spectrum is indicated on each pattern.



teristics of each group are presented. This paper does not intend to give definitive interpretations about the processes responsible for the appearance of these regularities. We will, however, briefly discuss the mechanisms possibly involved in these processes in order to better understand the real significance and extent of the XLT regularities.

"SKARN AND CALCSILICATE"-TYPE  
(FIGS 1B AND 6A, RESP.)

The scheelites associated to co-genetic calcsilicate rocks are characterised by a pronounced SB. Ac-

cording to our world-wide database, the Eu and Mo-contents may vary widely. The total REE content is low, and LREE are very enriched relative to HREE.

The very characteristic XLT spectra of these scheelites are related to the incorporation of REE by Ca-silicates, thereby decreasing the overall total REE content, and to preferential incorporation of HREE by garnets and pyroxenes (LIPIN and MCKAY, 1989), resulting in the enrichment of scheelite by LREE. Thus, the same XLT spectra are observed in scheelite from calcsilicates forming during contact metamorphic ("skarn") or during regional metamorphism.

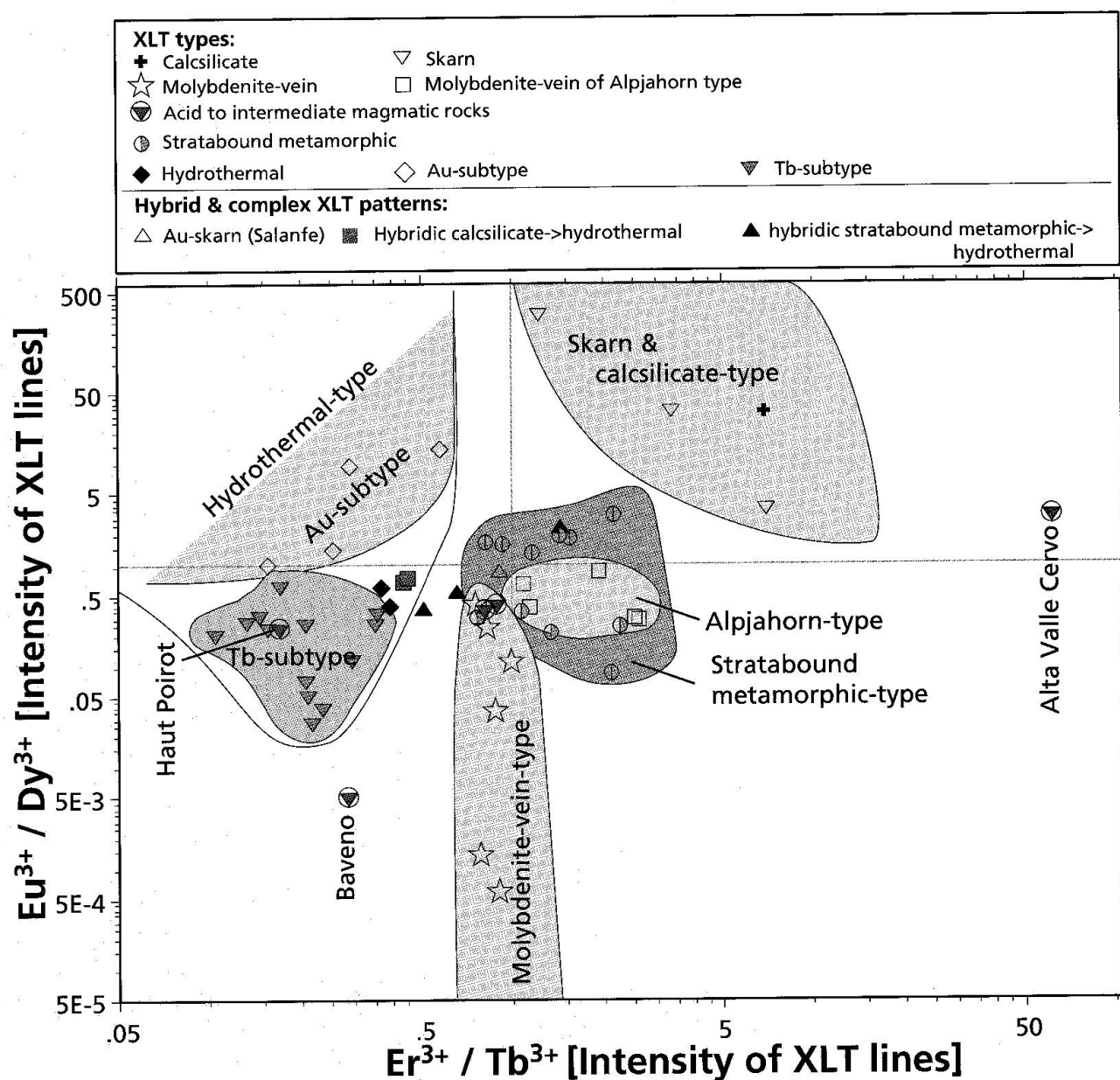



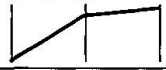


Fig. 5  $\text{Eu}^{3+}/\text{Dy}^{3+}$  versus  $\text{Er}^{3+}/\text{Tb}^{3+}$  (intensities of XLT characteristic peaks) variation diagram using XLT-data of scheelites from the Alps.



Tab. 4 Distinctive characteristics of the recognised XLT-spectra groups.

Type	Er <sup>3+</sup> -Tb <sup>3+</sup> -Dy <sup>3+</sup>	Mo*	Sm <sup>3+</sup> /Er <sup>3+</sup>	other characteristics	Fig.
<b>Skarn and calcsilicates</b>	these lines are often absent	often ↗	>> 1	high SB, low REE <sub>tot</sub>	1b 6a
<b>Molybdenite-vein</b> "True" molybdenite-vein		↗	> 1	Eu <sup>3+</sup> /Dy <sup>3+</sup> < 0.5	6b
Exceptions: Alpjahorn-type	Similar to "stratabound metamorphic" type		< 1	Significant Sm <sup>3+</sup> peak present	6c
<b>Acid to intermediate magmatic rocks</b>	highly variable	often ↗	> 1		6d
<b>Stratabound metamorphic</b>		↘	<< 1	Usually Eu <sup>3+</sup> < Dy <sup>3+</sup> Sm <sup>3+</sup> peak usually absent	6e
<b>Hydrothermal type</b>		↘	≥ 1		7a
Tb-subtype		↘	≥ 1	Exceptionally: Tb <sup>3+</sup> > Dy <sup>3+</sup> (7c)	7b/d, (7c)
Au-subtype		↘	≥ 1	Eu <sup>3+</sup> > Dy <sup>3+</sup>	7e
Au-subtype, High Eu differentiation		↘	≥ 1	Eu <sup>3+</sup> >> Dy <sup>3+</sup>	7f
Elevated SB type (scheelite redeposited in a vug)	reflects the spectrum of the source scheelite	↘	reflects the spectrum of the source scheelite	very high SB	7g/h

NOTES: (\*) ↘ means blue colour of visual luminescence (< 0.1 wt% Mo), ↗ yellow colour of visual luminescence. A typical spectrum for each type is indicated by the column "Fig.".

#### "MOLYBDENITE-VEIN" TYPE: SCHEELITE FROM MOLYBDENITE-APLITES (FIG. 6B) AND QUARTZ-MOLYBDENITE-VEINS (FIG. 2C)

##### Homogeneous, well characterised group

- (i) relatively high LREE;
- (ii) Er<sup>3+</sup> < Tb<sup>3+</sup> << Dy<sup>3+</sup>;
- (iii) Eu<sup>3+</sup>/Dy<sup>3+</sup> << 0.5;
- (iv) elevated Mo content.

Compared with that from molybdenite-aplites, scheelite from molybdenite-quartz veins usually displays slightly increased Tb<sup>3+</sup> and slightly decreased LREE<sup>3+</sup> peaks.

The samples from the Traversella skarn, and from the Bedovina W-Cu-(Mo,Sb) vein, are close to the "molybdenite-vein" type, with the exception of a higher Eu<sup>3+</sup> peak.

Our database shows that scheelites from molybdenite-aplites and quartz-veins form a very homogeneous group with respect to their XLT-spectra. These deposits are related to late mag-

matic processes near granitic or granodioritic intrusions. Therefore, the observed similarities in the spectra may result (i) from a similar source for fluids and metals and/or (ii) from a similar "transport medium", i.e., same complexes, Eh, etc. Similar mechanisms could be responsible for the deposition of the scheelite from the Traversella skarn.

##### Exceptions to the "molybdenite-vein" type: "Alpjahorn" type (Fig. 6c)

Several Mo-aplites and related veins have, however, spectra (Fig. 6c) very different from the usual "molybdenite-vein" type, but which are nearly identical to the "stratabound metamorphic" type (Fig. 6e). The molybdenite deposit of Alpjahorn (Baltshiedertal, VS) and some molybdenite-bearing quartz veins in the Bergell intrusives are the only localities which showed such spectra.

The nearly "stratabound metamorphic"-type XLT pattern for "Alpjahorn"-type scheelites sug-

gests a link between the scheelite found in the veins and scheelite of metamorphic stratabound deposits. The low Mo-content can be explained by a late stage crystallisation, Mo having been removed as molybdenite earlier in the crystallisation sequence.

"ACID TO INTERMEDIATE MAGMATIC ROCKS"-TYPE (FIG. 6D)

This group was created to account for some samples, all related to acid or intermediate magmatic rocks, which plot far away from the fields defined

in Fig. 5, or which plot in existing fields but display additional characteristics incompatible with this field. All these scheelites are characterised by the large size of the  $\text{Sm}^{3+}$  and  $\text{Pr}^{3+}$  peaks ( $\text{Sm}^{3+} > \text{Er}^{3+}$ ), which reflects the LREE enrichment typical of acid to intermediate magmatic rocks. "Molybdenite-vein" type scheelite may, in this regard, be considered as subtypes of the "acid to intermediate magmatic rock" type.

Baveno and Alta Valle Cervo scheelites plot outside any defined field (Fig. 5). The scheelite from a pegmatite pocket within the Baveno granite has low Mo-content,  $\text{Er}^{3+} < \text{Tb}^{3+} < \text{Dy}^{3+}$ , and  $\text{Eu}^{3+}/\text{Dy}^{3+} < 0.1$  (SLT66, Fig. 6d). So far, similar

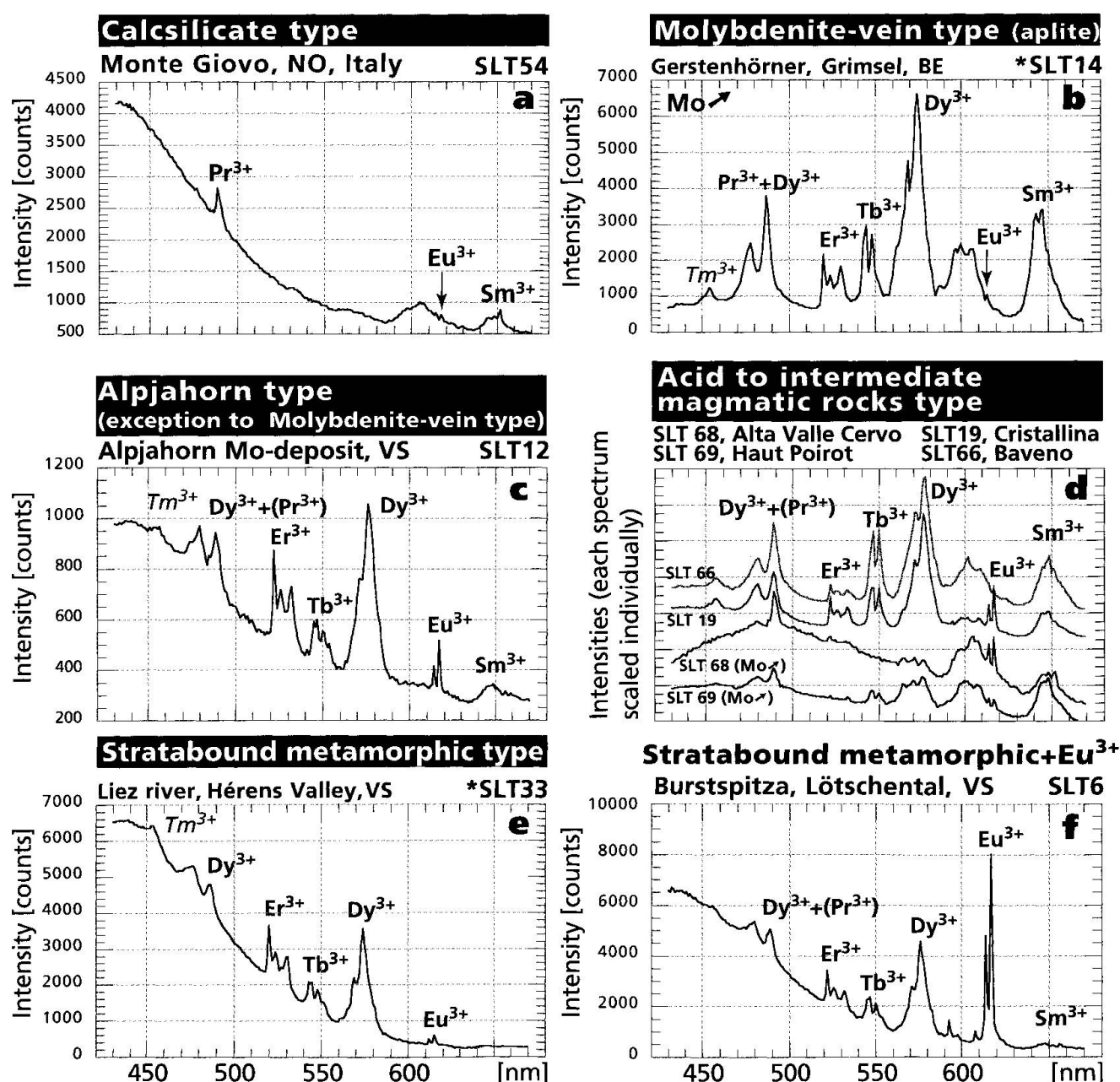


Fig. 6 XLT spectra of scheelites from the Alps, representative of the XLT-types listed in table 4.

spectra have been found only in two tin vein deposits (Viloco, Bolivia; Iultin, Chukotka, Russia), where scheelite is associated with cassiterite and wolframite in quartz veins. The scheelite from Alta Valle Cervo (SLT68, Fig. 6d) contains > 0.1

wt% Mo (SB maximum between 480 and 500 nm on the XL spectrum), and its XLT spectrum shows a  $Tb^{3+} \ll Dy^{3+} \approx Er^{3+}$  distribution and, among the LREE,  $Pr^{3+} > Sm^{3+}$ . In our database, some samples from pegmatites have similar features.

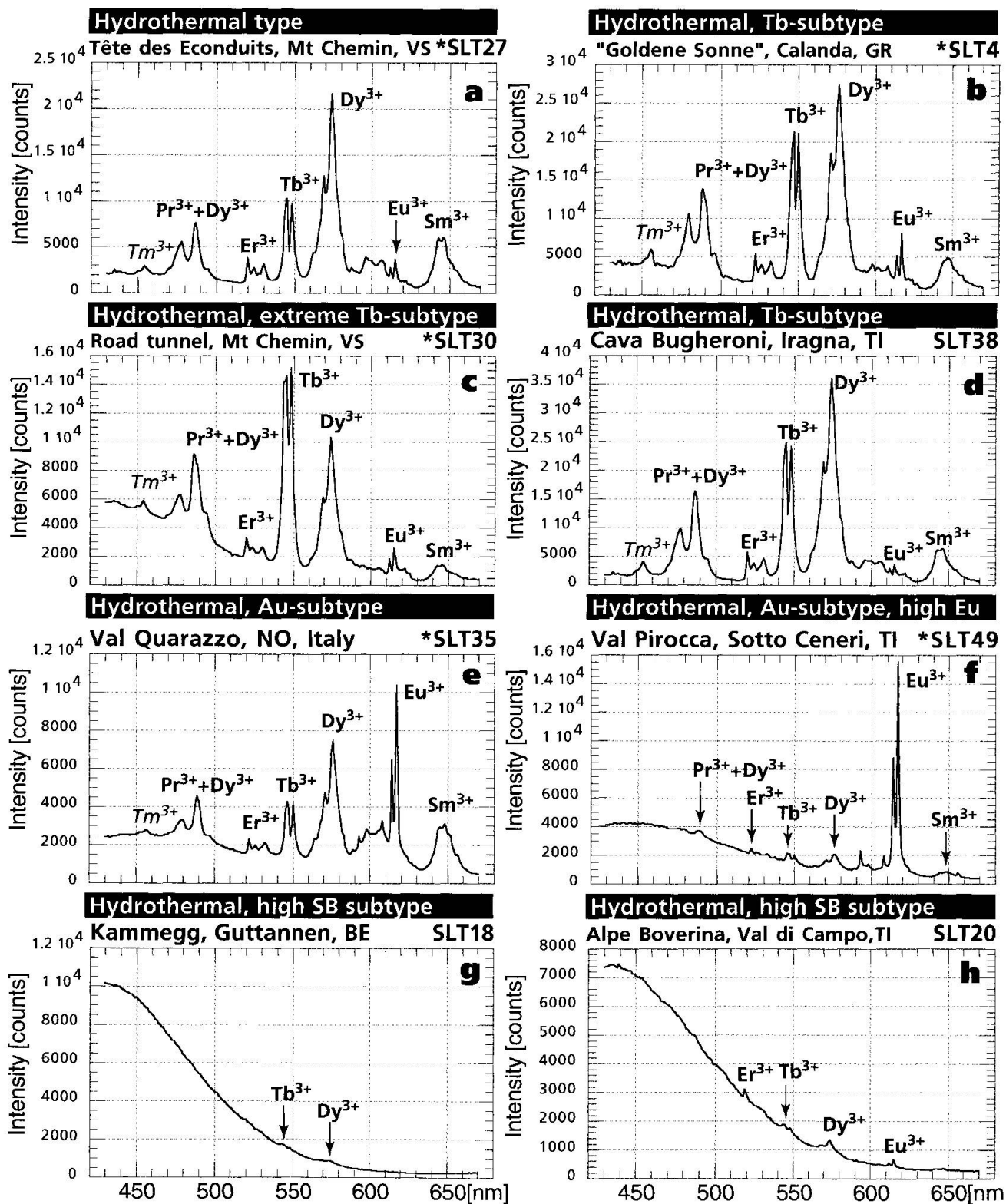


Fig. 7 Different kinds of XLT spectra of scheelites from hydrothermal settings in the Alps. The types according to table 4 are indicated.

The scheelite from Haut Poirot (SLT69, Fig. 6d) plots in the "hydrothermal, Tb-subtype" field, but is characterised by a very high  $\text{Sm}^{3+}$  peak, and by a high Mo-content (0.1–1 wt% according to luminescence colour). The scheelites from a shear zone within the St. Maria-Cristallina granodiorite (SLT19, Fig. 6d), and from a quartz vein (pegmatitic?) from Campra are very similar, with XLT characteristics between "hydrothermal" and "molybdenite-vein" types. Both samples have < 0.1 wt% Mo. Similar spectra within our database were found in scheelites from some Cu–Mo–(W), Cu–(W) and Cu–Mo–polymetallic ores.

The variety of spectra found in scheelite closely associated to magmatic rocks may represent remobilisation of tungsten enriched by magmatic processes, by different late magmatic (pegmatitic) to hydrothermal (Ht Poirot) and metamorphic (St. Maria-Cristallina) processes. The study of additional samples from similar settings may lead to the definition of new XLT-groups.

#### "STRATABOUND METAMORPHIC" TYPE (FIG. 6E)

XLT spectra of scheelite from metamorphic stratabound deposits (Fig. 6e) are characterised by low LREE and by the  $\text{Tb}^{3+} < \text{Er}^{3+} < \text{Dy}^{3+}$  distribution. They usually display  $\text{Eu}^{3+} \leq \text{Dy}^{3+}$ , and low Mo-content. Samples from Burstspitze (Lötschental, VS) (Fig. 6f) however, display  $\text{Eu}^{3+} \gg \text{Dy}^{3+}$  (compare with Val Firinesco, Sotto Ceneri: Figs 4f and 9f). The scheelite from Salanfeskarn falls in the metamorphic field (Fig. 10c), but also has elevated  $\text{Eu}^{3+}$ .

#### "HYDROTHERMAL" TYPE (FIG. 7)

All the spectra of figure 7 belong to hydrothermal scheelites. General characteristics include (Fig. 7a):

- (i) the  $\text{Er}^{3+} < \text{Tb}^{3+} < \text{Dy}^{3+}$  distribution
- (ii) low Mo-content.

#### "Hydrothermal" type, "Tb"-subtype (Fig. 7b)

Some hydrothermal scheelites are characterised by elevated  $\text{Tb}^{3+}$  peak ( $\text{Er}^{3+} \ll \text{Tb}^{3+} \leq \text{Dy}^{3+}$ ): Fig. 7b/d. They are relatively rare and have been found in Swiss Alpine vugs (Mt Chemin, Iragna), in the Swiss Au-deposits of Calanda and Disentis, in the Mn-vein of Haut Poirot (France), and in two Tertiary deposits connected to large scale faults in Bolivia and New Zealand. XLT spectra displaying

$\text{Tb}^{3+} > \text{Dy}^{3+}$  were only found at Mt Chemin, VS (Fig. 7c).

#### "Hydrothermal type, Au-subtype" (Figs 7e, f)

The XLT spectrum representative of scheelite from Au-vein (Fig. 7e) shows typical hydrothermal features ( $\text{Er}^{3+} < \text{Tb}^{3+} < \text{Dy}^{3+}$  distribution) but has a high  $\text{Eu}^{3+}/\text{Dy}^{3+}$  ratio. The spectrum 8f is similar, but with very high  $\text{Eu}^{3+}$  peak (Au-subtype, high degree of Eu-differentiation). The latter type is relatively rare within our world-wide database, and is always found in Au-ores.

USPENSKY et al. (1990) first suggested that high positive Eu-anomalies are characteristic for scheelite from Au-deposits of various age, genetic type, and localisation. In the Alps, high positive Eu anomalies were described in scheelite from the Au-deposits of Val Toppa, Italy (RICHARD et al., 1981), and Schellgaden, Austria (IVANOVA and POTY, 1992). XLT spectra of scheelites from the Au-ores of Val Toppa and Val Quarazzo, Italy (Figs 4c, 7e) are characteristic of their hydrothermal origin ( $\text{Er}^{3+} < \text{Tb}^{3+} < \text{Dy}^{3+}$ ), and additionally exhibit  $\text{Eu}^{3+}/\text{Dy}^{3+} > 1$ , thus conforming with the usual feature.

It should be mentioned that scheelite from the Calanda Au-deposit shows only a small  $\text{Eu}^{3+}$ -peak in the XLT-spectrum (Fig. 7b), which corresponds to a negative Eu-anomaly on the chondrite normalised plot (Fig. 4i). This example illustrates that if scheelite with high  $\text{Eu}^{3+}/\text{Dy}^{3+}$  were always found within Au-bearing mineralisations, not all the scheelites from this kind of ores displayed this feature.

#### "Elevated SB" type (Figs 7 g, h)

Spectra of scheelite from "Alpine vugs" usually display a very large SB, which almost obliterates the characteristic peaks even on the XLT spectrum, although the latter represents a quenching of the SB by a factor 15 relative to the XL spectrum. When they were measurable, the line patterns resembled some of the types already mentioned.

At Alpe di Boverina and Kammegg, scheelite crystals occur in Alpine vugs without connection to any known W-mineralisation. The elevated SB carries small  $\text{REE}^{3+}$  peaks characteristic of the "stratabound metamorphic type" at Alpe Boverina (Fig. 7h) and of the "hydrothermal type" at Kammegg (Fig. 7g). The brown, transparent, euhedral scheelite crystals from vugs of Miniera di Brosso (Italy) have a XLT spectrum similar to

that of the Kammegg scheelite, with an additional small  $\text{Eu}^{3+}$ -peak in the spectrum.

The increase in lattice defects reflected by the high SB common in scheelite from open vugs reflects the condition of crystal growth in this environment, and may be caused by high speed of crystallisation, or by high levels of impurities (high W and Ca over impurity ratios in the solution).

#### "Hydrothermal" type: case study at Mt Chemin

Scheelite from quartz-epidote-amphibole veinlets crosscutting the Fe-skarv in Couloir Collaud has a typical "stratabound metamorphic" XLT pattern ( $\text{Er}^{3+} \gg \text{Tb}^{3+}$ ; low LREE and  $\text{Eu}^{3+}$ ; e.g., Fig. 6e – Liez River). However, this scheelite displays some unusual features: (i) increase of SB (bright blue visual luminescence); (ii) lack of colour; (iii) significant decrease in total REE. These features are considered to be typical for a scheelite redeposited from a primary metamorphic scheelite, al-

though true "stratabound metamorphic"-type scheelite has not yet been found in this area.

The other scheelites from Mt Chemin, which were collected in different geological settings within a limited area of about 2 km<sup>2</sup>, have the XLT spectra typical of their hydrothermal genesis ( $\text{Er}^{3+} \ll \text{Dy}^{3+}$ ), but they are characterised by a large variation in the  $\text{Tb}^{3+}/\text{Dy}^{3+}$  ratio which contrasts with the stable  $\text{Er}^{3+}/\text{Dy}^{3+}$  ratio (Fig. 8).  $\text{Eu}^{3+}/\text{Dy}^{3+}$  and  $\text{Sm}^{3+}/\text{Dy}^{3+}$  show small variations, and the increase of the complex peak ( $\text{Pr}^{3+} + \text{Dy}^{3+}$ ) correlates with that of the  $\text{Tb}^{3+}$  peak. In fact, a complete series of spectra exists from usual hydrothermal scheelite ( $\text{Er}^{3+} < \text{Tb}^{3+} < \text{Dy}^{3+}$ , SLT31) to a very unusual type ( $\text{Er}^{3+} \ll \text{Dy}^{3+} < \text{Tb}^{3+}$ , SLT30), with  $\text{Tb}^{3+}/\text{Dy}^{3+} > 1$ .

The chondrite-normalised plots of REE for samples SLT30 (Fig. 4g) and SLT27 (Fig. 4h) show "broad hump"-type curves, accompanied by negative Eu anomalies. Tb cannot be determined by ID method, but it is clear that SLT30 has a maximum between Gd and Dy (Tb-position), whereas the maximum for sample SLT27 is located near Sm. Therefore, at least part of the change in the Tb/Dy XLT peaks ratio is related to a smooth shift of the chondrite normalised plot maximum from SLT31 to SLT30.

The XLT data therefore allow to recognise a continuity between the various scheelite occurrences at Mt Chemin. The  $\text{Tb}^{3+}/\text{Dy}^{3+}$  variability at this locality is a unique feature.

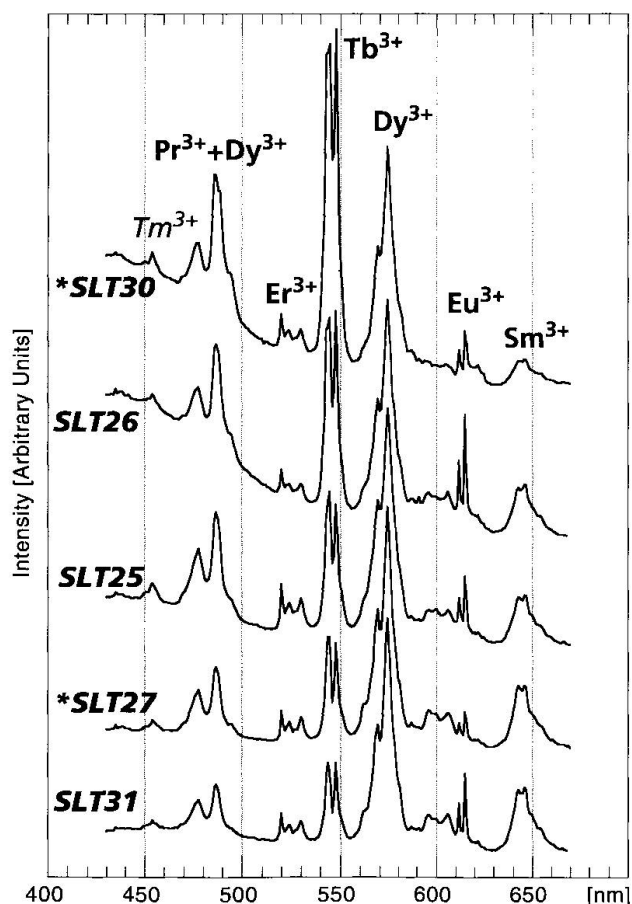


Fig. 8 Comparison of XLT spectra of scheelites from different settings at Mt Chemin near Martigny (VS, Switzerland). The intensity scales of each spectrum have been fixed individually to obtain equal  $\text{Dy}^{3+}$  peaks.

#### Applications of the XLT method to the study of Au-deposits

This section illustrates how the XLT method can be applied to the study of single deposits and/or provinces. In particular, the possibility to recognise complex (hybrid) patterns is explored.

#### SOTTO CENERI AND BURSTSPITZA

Primary metamorphic scheelite in Sotto Ceneri is often dispersed and fine-grained, and most analysed scheelites therefore come from small discordant veinlets crosscutting gneisses and calc-silicate rocks, and containing coarser and more abundant scheelite. Some of these scheelites, however, display XLT spectra of "calc-silicate" (Fig. 9a) and "stratabound metamorphic" (Fig. 9b) types, in agreement with the stratabound metamorphic nature of this mineralisation. Additionally, some samples yielded spectra ranging from "hydrothermal" (Fig. 9c) to "Au-subtype with high degree of Eu differentiation" (Fig. 9d), and



many kinds of hybrid XLT patterns have been determined. For example, the spectrum 10e could represent the mixing of "calcsilicate type" with "hydrothermal type", and 10f the mixing of "stratabound metamorphic type" with "Au-subtype with high degree of Eu differentiation".

This kind of hybridisation is recognisable also on chondrite normalised patterns. Hybrid scheelite from Val Firinesco (Fig. 4f) has a positive Eu-anomaly, and displays a relatively "hydrothermal" type of curve between La and Sm (compare with Val Quarazzo; Fig. 4c), but HREE are somewhat increased. The normalised plot of Val Pirocca scheelite displays similar characteristics (Fig. 4e). The enrichment of HREE is, however, typical for "stratabound metamorphic type" scheelites (Fig. 4a).

These data suggest that the stratabound, metamorphic scheelite has been partly remobilised during a large scale hydrothermal event, which may be correlated with the numerous, often Au-bearing hydrothermal veins of Malcantone. These veins are devoid of scheelite (WENGER, 1987). However, it should be noted that the sample with highest positive Eu-anomaly comes from Val Pirocca, which is close (< 1 km) to three different Au-bearing veins (KÖPPEL, 1966).

Scheelites from Burstspitze, Lötschental, VS, where W is associated with a Bi-Ag ± Pb anomaly, show hybrid XLT patterns with significant variations in  $\text{Eu}^{3+}/\text{Dy}^{3+}$ , similar to the ones from Sotto Ceneri (compare Figs 6f and 9f). These patterns suggest hydrothermal remobilisation of "stratabound metamorphic" and "calcsilicate"

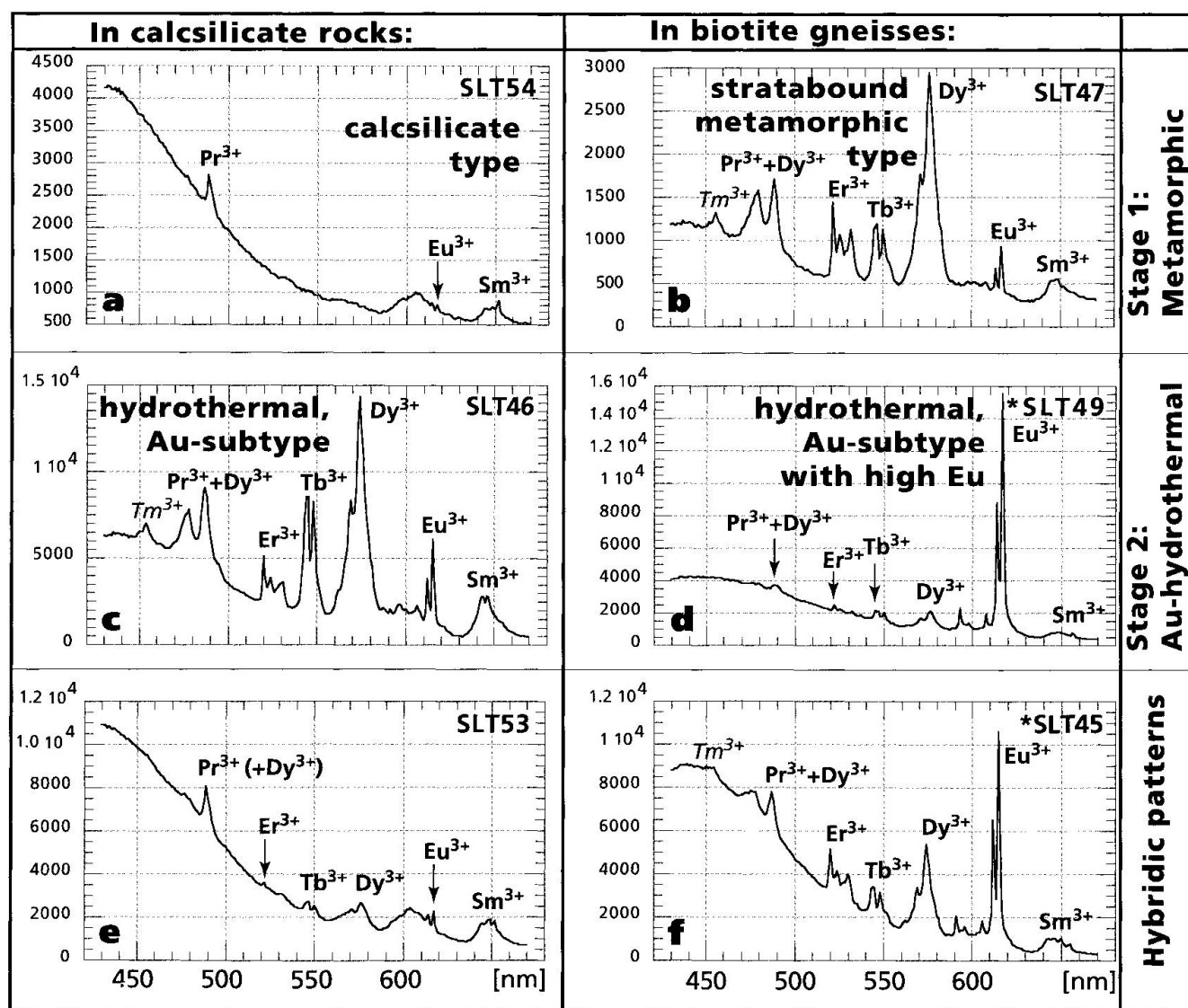


Fig. 9 Different types of XLT spectra of scheelites from Sotto Ceneri (Switzerland and Italy). Vertical axes are intensities [counts]. The complexity of the spectra collected in these scheelites may be explained by hydrothermal remobilisation of a stratabound scheelite mineralisation.

type scheelite. As there is no indication as to the presence of Au in this area, no conclusion can be made at this stage. Nevertheless, these results can be used as a basis for more detailed mapping and Au-prospecting.

#### SALANFE AND THE Au-SKARNS

XLT spectra of scheelites from some Au-bearing skarns are reported in figure 10. Figure 10a is typical for scheelite from calcsilicate rocks. The scheelite from Salanfe, however, is very different (Fig. 10c). It shows an elevated  $\text{Eu}^{3+}$  peak ( $\text{Eu}^{3+} \approx \text{Dy}^{3+}$ ),  $\text{Er}^{3+}$ - $\text{Tb}^{3+}$ - $\text{Dy}^{3+}$  distribution similar to "stratabound metamorphic" type, but with relatively elevated light part and a  $\text{Tb}^{3+}$  peak slightly higher than the  $\text{Er}^{3+}$  peak (i.e. approaching the "hydrothermal" type). Similar spectra have been found in some scheelites from the French Au-skarns Costabonne (Fig. 10b) and Salau (Fig. 10d). The chondrite-normalised plot for Salanfe scheelite (Fig. 4d) shows a "broad-hump"-like curve with a small negative Eu-anomaly. The shape of the curve is typical for "hydrothermal" scheelites, but the total REE concentration is lower at Salanfe than in typical "hydrothermal" scheelites. The XLT spectrum of the Salau scheelite is more similar to the "hydrothermal, Au-subtype" type:

low Mo-content,  $\text{Er}^{3+} < \text{Tb}^{3+} < \text{Dy}^{3+}$ , and  $\text{Eu}^{3+}/\text{Dy}^{3+} > 2$ , which is consistent with the positive Eu-anomaly visible on the chondrite-normalised plot published by RAIMBAULT et al. (1993).

It should be emphasised that XLT-spectra of scheelites from Au-skarns, first of all Costabonne (Fig. 10b) and Salanfe (Fig. 10c), are very similar to those from Burstspitz (Fig. 6f) and the hybrid samples from Sotto Ceneri (Fig. 9f).

Scheelite from the Luisin occurrence, situated relatively near to Salanfe (1 km), has a very high degree of Eu-differentiation (only the  $\text{Eu}^{3+}$  peak is seen in the XLT-spectrum), but very low total REE content (the  $\text{Eu}^{3+}$  peak is very small). XLT patterns of this type are found in scheelite associated with the margins of some Au-deposits.

The Luisin scheelite suggests that the Au-related event that produced Au deposition at Salanfe could have a regional importance. XLT mapping of the scheelite occurrence in that region could help to constrain such a supposition.

In general, these observations on Au-bearing skarns confirm the existence of a global phenomenon, which acted among most Au-ores, and whose appearance is most likely related to some physico-chemical characteristics of the early solutions. At Salanfe scheelite precipitates shortly before the precipitation of Au-bearing sulphides, indicating that XLT spectra of scheelite may contain information about the evolution of the minerali-

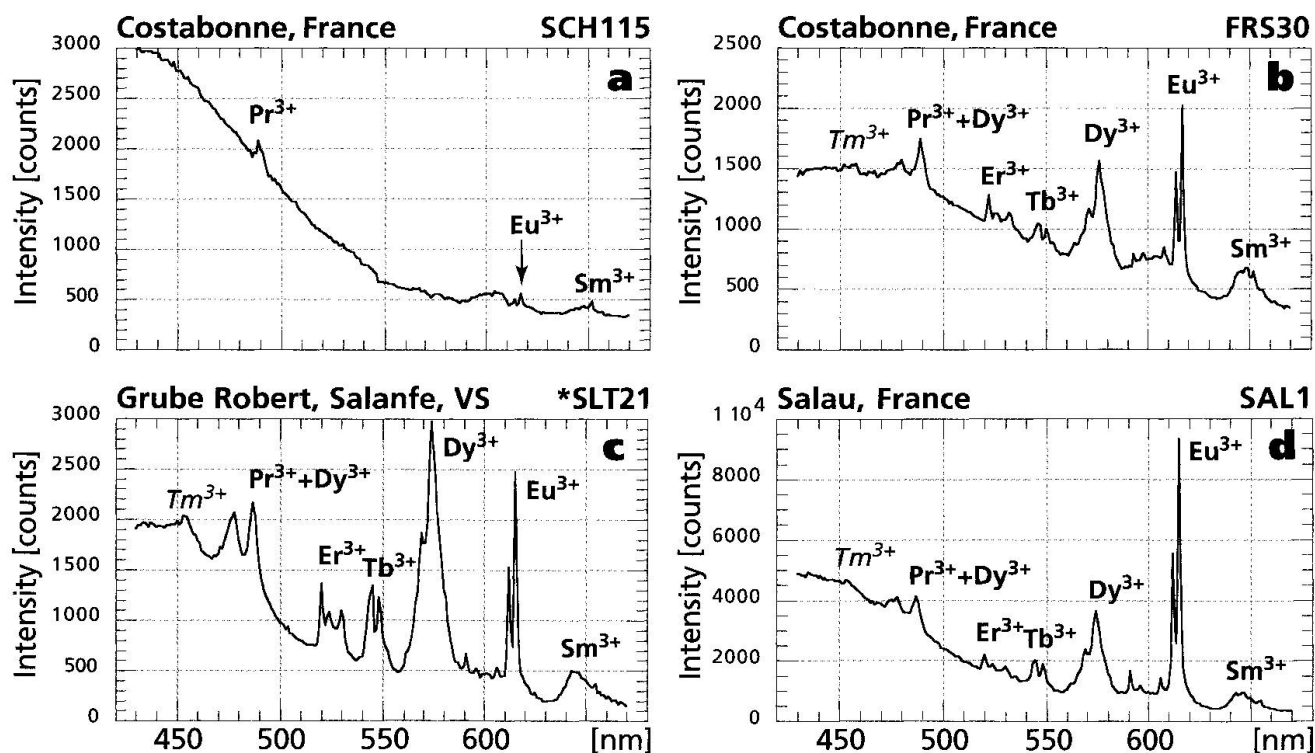


Fig. 10 XLT spectra of scheelites from gold skarns.

sation. Detailed study of deposits such as Costabonne, where a "normal" skarn scheelite and a "Au-skarn" scheelite coexist, are important in order to constrain better the factors controlling the changes to the scheelite XLT-patterns.

### DISENTIS

The XLT method is able to analyse quickly and accurately even small single scheelite grains (0.2–0.5 mm). Scheelite is commonly encountered in heavy mineral concentrates (HMC), and in this section we demonstrate how XLT studies of placer scheelite can be used as a prospecting tool for lode deposits.

Scheelite grains (0.2–1.5 mm) were collected in Au-bearing HMC from the Medel river near Disentis. The scheelite grains can be divided into three groups on the basis of their macroscopic colour, UV-luminescence, and XLT spectra:

(I) light yellow coloured grains with blue visual luminescence under UV-lamp (VL); 60% of the scheelite in the HMC. The XLT spectrum (Fig. 11a) is of "hydrothermal" type ( $\text{Er}^{3+} < \text{Tb}^{3+} < \text{Dy}^{3+}$ ) and displays high  $\text{Eu}^{3+}/\text{Dy}^{3+}$  ratios ("hydrothermal, Au-subtype with high Eu differentiation"). This scheelite is undoubtedly related to Au-ores.

(II) transparent, colourless grains with bright blue VL; 10% of HMC scheelite. The XLT spec-

trum (Fig. 11b) reveals the same high degree of Eu-differentiation as (I), but has increased SB, and (ii) a significantly higher  $\text{Tb}^{3+}$  peak ( $\text{Er}^{3+} \ll \text{Tb}^{3+} \approx \text{Dy}^{3+}$ ).

(III) white/greyish-white coloured grains with yellow VL (corresponding to about 0.1–0.9 wt% Mo); 30% of HMC scheelite. Their XLT spectra (Fig. 11c) are of "molybdenite-vein" type.

Thus, the XLT-data on HMC from Disentis can distinguish two main types of scheelite apparently corresponding to different lode ores: (i) hydrothermal Au-ores; (ii) molybdenite-aplites (molybdenite-quartz-veins?). Transparent grains with a high SB similar to group II usually have been observed in Alpine vugs. The similarity of the XLT patterns of groups I and II suggests that scheelite II was formed by remobilisation of primary scheelite I, "Au-subtype with high degree of Eu differentiation" during the Alpine metamorphism. The same event could be responsible for the neoformation of gold crystals in quartz-bearing Alpine vugs. The origin of "molybdenite-vein" type scheelites (group III) is likely to be the Aar-Massif, in which many molybdenite-aplites are described.

The occurrence of scheelite with "hydrothermal, Au-subtype with high Eu differentiation" XLT spectrum at Disentis is important, because similar spectra have up to date been found only in scheelite closely associated to ores with high Au-contents (> 10 g/t). The recognition that Au-min-

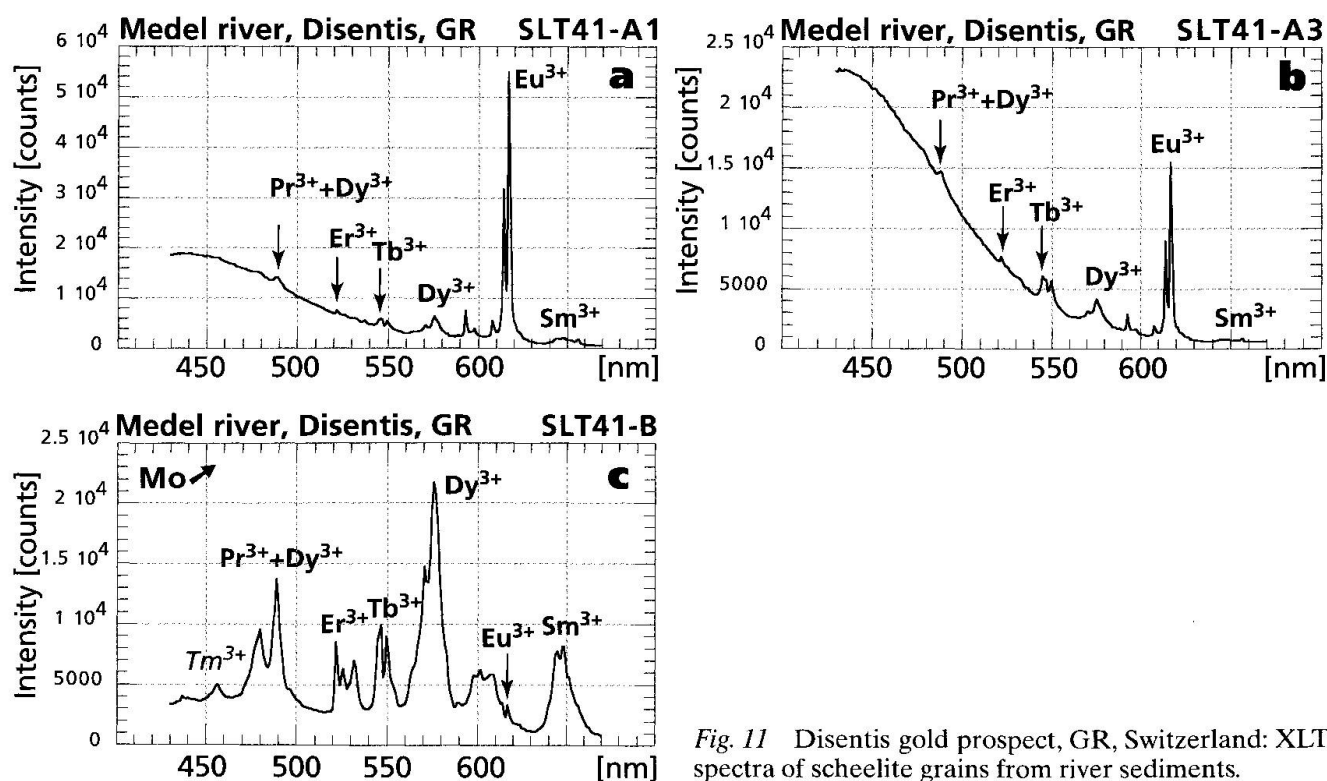


Fig. 11 Disentis gold prospect, GR, Switzerland: XLT spectra of scheelite grains from river sediments.

eralisation is associated with scheelite will assist future prospecting.

### Conclusions

The advantages of the XLT spectroscopic method include high sensitivity to the trace element content of scheelite, small sample size, and the selective analysis of the REE<sup>3+</sup> substituting for Ca in the scheelite lattice, thus avoiding a careful study of micro-inclusions in scheelite. Our qualitative approach proved to be successful in recognising some common features among the XLT-spectra of scheelites from deposits with similar metallogenic type. The following scheelite types have been defined on the basis of the XLT patterns: "calcsilicate/skarn", "molybdenite-vein", "acid to intermediate magmatic rocks", "stratabound metamorphic", "hydrothermal", "hydrothermal, Tb-subtype", "hydrothermal, elevated SB-subtype", "hydrothermal, Au-subtype" evolving to "Au-subtype with high Eu differentiation". The comparison of the 70 samples from the Alps with our world-wide XLT spectra database (yet unpublished) indicates the global nature of these characteristic patterns.

A very important parameter used to discriminate the groups is the Er<sup>3+</sup>-Tb<sup>3+</sup>-Dy<sup>3+</sup> triplet, which is very sensitive to the shape and pattern of the chondrite normalised REE plot, a parameter usually neglected by most studies. Many studies of REE in hydrothermal minerals stress the local influences (e.g., influence of host rocks, of competition with other species, etc.), but the recognition of global features leads to a new approach towards understanding the REE geochemistry of hydrothermal systems, and prospecting for new ore bodies.

The technique has been applied to the study of single deposits and provinces associated with Au-mineralisations from the Alps. Complex (hybrid) REE-patterns were recognised in the Sotto Ceneri area using the XLT method. Such XLT patterns can help to understand the complex processes of ore re-deposition, to assess the scale of hydrothermal events, and to identify different stages of ore formation. The XLT method is well suited for large scale mapping of the trace element characteristics of scheelite: such maps have the potential to visualise the extend of hydrothermal events and, in the case of Au-deposits, to define the more promising mineralised zones, as scheelite with very high Eu<sup>3+</sup>/Dy<sup>3+</sup> peak ratios were always found in high grade ores.

The data collected on scheelite grains from river sediments of Disentis show that much informa-

tion about the metallogeny of the region can be obtained: in that example the existence of Au-mineralisation, which was reworked at Alpine time, and of a separate Mo-mineralisation were identified. Thus, XLT is a very powerful complementary method in association with the prospecting using heavy mineral concentrates.

The XLT method is also useful as a preliminary step for detailed geochemical investigations of scheelite. In the various examples presented in this paper, XLT was able to classify the scheelite samples, and to indicate the samples and localities with unusual features. A model explaining the observations may often be derived from the XLT data. Testing such a model requires careful petrographic investigations coupled with isotopic analyses and quantitative trace elements determinations. The latter should be carried out with spatially resolved methods, such as laser ablation ICP-MS, which allow to investigate the nature and morphology of the chemical heterogeneities at the scale of a scheelite grain. Applied to scheelites displaying "hybrid" XLT-spectra, this approach would for example allow to determine if the hybrid patterns correspond to homogeneous compositions or if they result from a mixture of two different scheelites. This kind of investigations, however, is time and resource consuming, and the XLT method is of great help by allowing to select the more informative samples, and to set up a working hypothesis.

### Acknowledgements

We are grateful to the "Freiwillige Akademische Gesellschaft" of Basel for supporting this project financially, to O. Kononov (Moscow University) for advice on the preparation of synthetic scheelite standards, and to D.Z. Zuravlev (IGEM Russian Academy of Sciences) for the ID analyses. Many improvements to the manuscript arose from the comments of R. Gieré (Purdue University, Indiana) and M. Chiaradia (Geneva University). The manuscript also greatly benefited of the thorough reviews of Terry Williams and Viktor Köppel.

We would like to thank all the people and institutions who gave us scheelite samples, in particular S. Ansermet (La Tour de Peilz) and A. Salzmann (Vevey), who carried out a very careful prospecting work at Mt Chemin, Hans-Ruedi Rüegg (Basel), who furnished the scheelite from the HMC from Disentis, and W. Paar (Salzburg University), who has provided scheelites from Austrian deposits and from Bedovina. Special thanks to Beda Hofman and Nicolas Meisser, who opened us the doors of the museums of Bern and Lausanne, respectively. Further samples were generously provided by Stefan Graeser (Nat. Hist. Museum Basel), Franco Vaini (Varese, Italy), Claudio Albertini (Omegna, Italy), Roger Zurbruggen (Min. Petr. Inst., Bern University),



the Institute of Mineralogy and Petrography of Fribourg (coll. UROMINE), and the Institute of Mineralogy and Petrography of Bern (Coll. Wenger).

### References

- ANGLIN, C.D. (1990): Preliminary Sm-Nd isotopic analyses of scheelites from Val d'Or gold deposits, Quebec. *Pap. Geol. Surv. Can.* 90-1C, 255-259.
- AUDÉTAT, A. (1995): Mineralogische und petrographische Untersuchungen an Au-, Sb-, Cu-führenden Quarz-Karbonat-Gängen am Calanda bei Chur, Kt. Graubünden. Unpublished diploma thesis, Institut für Mineralogie und Petrographie, ETH Zürich.
- BÄCHTIGER, K. (1974): Die alpidische Gold-Wolfram-Vererzung am Calanda bei Chur. *Fortschr. Min.* 52, Beiheft 2, 3-5.
- BÄCHTIGER, K., RÜDLINGER, G. and CABALZAR, W. (1972): Scheelit in Quarz- und Fluorit-Gängen am Calanda (Kt. Graubünden). *Schweiz. Mineral. Petrogr. Mitt.* 52, 561-563.
- BAU, M. (1991): Rare-earth element mobility during hydrothermal and metamorphic fluid-rock interaction and the significance of the oxidation state of europium. *Chemical Geology* 93, 219-230.
- BELL, K., ANGLIN, C.D. and FRANKLIN, J.M. (1989): Sm-Nd and Rb-Sr isotope systematics of scheelites: possible implications for the age and genesis of vein-hosted gold deposits. *Geology* 17, 500-504.
- BIANCONI, F. and SIMONETTI, A. (1967): La brannerite e la sua paragenesi nelle pegmatiti di Lodrino. *Schweiz. Mineral. Petrogr. Mitt.* 47, 887-943.
- BUSSY, F. (1990): Pétrogenèse des inclusions microgrenues associées aux granitoides calco-alcalins: exemple des massifs varisques du Mont-Blanc (Alpes Occidentales) et miocènes du Monte Capanne (Ile d'Elbe, Italie). *Mémoires de Géologie (Lausanne)* N° 7, 309 pp.
- CARUBA, R., IACCONI, P., COTTRANT, J.F. and CALAS, G. (1983): Thermoluminescence, fluorescence and electron paramagnetic resonance properties of synthetic hydrothermal scheelites. *Phys. Chem. Minerals* 9, 5, 223-228.
- CHIARADIA, M. (1993): The scheelite skarn of Salanfe (Valais, Switzerland). Ph.D. Thesis, University of Fribourg, Switzerland.
- CHIARADIA, M. (1994): Sedimentary protoconcentrations as a source of tungsten in the W-As-Au skarn of Salanfe (Aiguilles Rouges Massif, Switzerland). *Schweiz. Mineral. Petrogr. Mitt.* 74, 329-342.
- COTTRANT, J.F. (1981): Cristallochimie et géochimie des terres rares dans la scheelite: Application à quelques gisements français. Ph.D. Thesis, University of Paris-VI, France.
- ENGEL, W., AMSTUTZ, G.C. and SCHAUFELBERGER, F. (1986): Zur petrographisch-lagerstättenkundlichen Stellung der Mo-W-Lagerstätte Alpjahorn, Wallis, Schweiz (Abstract). *Fortschr. Min.* 64, Beiheft 1, 43.
- EVENSEN, N.M., HAMILTON, P.J. and O'NIONS, R.K. (1978): Rare earth elements abundances in chondritic meteorites. *Geochim. Cosmochim. Acta* 42, 1199-1212.
- EXEL, R. (1993): Die Mineralien und Erzlagerstätten Österreichs. Eigenverlag Dr. Reinhard Exel, Wien, 447 pp.
- FINLOW-BATES, T. and TISCHLER, S.E. (1983): Controls on Alpidic mineralization styles. In: SCHNEIDER, H.-J. (ed.): *Mineral deposits of the Alps*. Springer Verlag, Berlin, Heidelberg, 7-18.
- FLEET, A.J. (1983): Hydrothermal and hydrogenous ferro-manganese deposits: do they form a continuum? The rare earth evidence. In: RONA, P.A., BOSTRÖM, K., LAUBIER, L. and SMITH, K.L. (eds): *Hydrothermal processes at seafloor spreading centers*. Nato Conf. Ss. IV, Plenum Press, New York, 535-556.
- FLUCK, P. and WEIL, R. (1975): Géologie des gîtes minéraux des Vosges et des régions limitrophes. *Mémoire du BRGM* 87, 73 pp.
- GIERÉ, R. (1996): Formation of rare earth minerals in hydrothermal systems. In: JONES, A.P., WALL, F. and WILLIAMS, T.C. (eds): *Rare Earth Minerals: chemistry, origin and ore deposits*. Chapman & Hall, London, 105-150.
- GIUSSANI, A. (1978): Skarn related mineralization in the magnetite-pyrite-hematite deposit of Brosso (Ivrea, Italy). *Verh. Geol. B-A. Proceed. 3rd ISMDA (Leoben, Oct. 7-10, 1977)*, 321-346.
- GRAESER, S. (1984): Die Mineralien des Strassentunnels Mittel-Hohtenn/V.S. *Schweiz. Strahler* 6, 12, 524-549.
- GRASSER, R. and SCHARMANN, A. (1976): Luminescent sites in  $\text{CaWO}_4$  and  $\text{CaWO}_4\cdot\text{Pb}$  crystals. *Journal of Luminescence* 12-13, 473-478.
- HANUZA, J., HERMANOWICZ, K., RYBA-ROMANOWSKI, W., DRULIS, H. and USPENSKY, E.I. (1994): Spectroscopy of Rare Earth (III) Ions in Natural  $\text{CaWO}_4$  Scheelite Minerals. *Polish J. Chem.* 68, 185-194.
- IVANOVA, G.F. and POTY, B. (1992): REE concentrations, forms and types of distribution in scheelites. *Geochem. Int.* 29, 12, 20-30.
- KEMPE, U., TRINKLER, M. and WOLF, D. (1991): Yttrium und die Seltenerdphotolumineszenz natürlicher Scheelite. *Chem. Erde* 51, 275-289.
- KENT, A.J.R., CAMPBELL, I.H. and MCCULLOCH, M.T. (1996): Sm-Nd systematics of hydrothermal scheelite from the Mount Charlotte mine, Kalgoorlie, Western Australia: an isotopic link between gold mineralization and komatiites. *Economic Geology* 90, 2329-2335.
- KNOPE, D.J., NAERT, K.A. and BELL, D.R. (1989): New type mineralisation in the Swiss Alps: the Disentis gold occurrence. *Mining Magazine* October, 290-296.
- KOEPPENKASTROP, D. and DE CARLO, E.H. (1992): Sorption of rare-earth elements from sea water onto synthetic mineral particles: An experimental approach. *Chemical Geology* 95, 251-263.
- KÖPPEL, V. (1966): Die Vererzungen im insubrischen Kristallin des Malcantone und geothermometrische Untersuchungen in Arsenkies-Zinkblende. *Beiträge zur Geologie der Schweiz, Geotechnische Serie*, 40. Lieferung, 132 pp.
- LIMARENKO, L.N., NOSENKO, A.E., PASHKOVSKY, M.B. and FUTORSKY, D.-L.L. (1978): The influence of structure's defects on physical properties of tungstates. Lvov: "Vistcha Skola", 160 pp.
- LIPIN, B.R. and MCKAY, G.A. (1989): Geochemistry and mineralogy of rare earth elements. *Reviews in Mineralogy*, 21. Mineralogical Society of America, 348 pp.
- LOTTERMOSER, B.G. (1992): Rare earth elements and hydrothermal ore formation processes. *Ore Geol. Rev.* 7, 1, 25-41.
- MARIANO, A.N. and RING, P.F. (1975): Europium-activated C-Luminescence in minerals. *Geochim. Cosmochim. Acta* 39, 649-660.
- MARSHALL, D. (1995): Alpine and Variscan pressure-temperature-time paths, N-E Mont Blanc Massif, Valais, Switzerland. Unpublished Ph. D. Thesis, University of Lausanne (CH).



- MAURIZIO, R. and MEISSER, N. (1993): Neue Mineralien des Bergells (Schweiz-Italien). *Schweiz. Strahler* Vol. 9, Nr. 11, 525–557.
- MEISSER, N. and ANSERMET, S. (1993): Topographie minéralogique de la Suisse et des pays voisins: description de minéraux rares ou inédits récemment découverts. *Le cristallier suisse* 9, 12, 573–590.
- MÖLLER, P. and MORTEANI, G. (1983): On the geochemical fractionation of rare earth elements during the formation of Ca-minerals and its application to problems of the genesis of ore deposits. In: AUGUSTITHIS, S.S. (ed.): *The significance of trace elements in solving petrogenetic problems and controversies*. Theophrastus Publications S.A., Athens, Greece.
- MÖLLER, P., MORTEANI, G. and DULSKI, P. (1984): The origin of the calcites from Pb–Zn veins in the Hartz Mountains, Federal Republic of Germany. *Chemical Geology* 45, 91–112.
- MÖLLER, P., PAREKH, P.P. and SCHEIDER, H.J. (1976): The application of Tb/Ca–Tb/La abundance ratios to problems of fluor spar genesis. *Mineral. Deposita* 11, 111–116.
- MORGAN, J.W. and WANDLESS, G.A. (1980): Rare earth element distribution in some hydrothermal minerals: evidence for crystallographic control. *Geochim. Cosmochim. Acta* 44, 973–980.
- PARKER, R.L. (1973): *Die Mineralfunde der Schweiz*. Neubearbeitung durch H.A. STALDER, F. de QUERVAIN, E. NIGGLI und S. GRAESER. Verlag Wepf & Co, Basel.
- RAIMBAULT, L., BAUMER, A., DUBRU, M., BENKERROU, C., CROZE, V. and ZAHM, A. (1993): REE fractionation between scheelite and apatite in hydrothermal conditions. *Amer. Mineral.* 78, 1275–1285.
- RAKOVAN, J. and REEDER, R. (1996): Intracrystalline rare earth element distribution in apatite – surface structural influences on incorporation during growth. *Geochim. Cosmochim. Acta* 60, 4435–4445.
- RAKOVAN, J. and REEDER, R.J. (1994): Differential incorporation of trace elements and dissymmetrization in apatite – the role of surface structure during growth. *Amer. Mineral.* 79, 892–903.
- RICHARD, A., DABROWSKI, H. and MICHEL, R. (1981): Contribution à l'étude des éléments en traces de quelques scheelites des Alpes. *Géologie Alpine* 57, 109–114.
- SEMENOV, Y.I. (1963): Rare earth mineralogy (in Russian). *Izd. AN SSSR, Moscow*, 412 pp.
- STALDER, H.A. and WENGER, C. (1988): Scheelit aus dem Aar- und Gotthardmassiv. *Schweiz. Strahler* 8, 2, 45–65.
- STELLA, A. (1943): I giacimenti auriferi delle Alpi Italiane. *Memorie descrittive della carta geologica d'Italia XXVII*, 1–134.
- TORONI, A. (1984): Scheelitkristalle aus der Alpe Boverina (Val di Campo) und Iragna. *Schweiz. Strahler* 6, 11.
- TYSON, R.M., HEMPHILL, W.R. and THEISEN, A.F. (1988): Effect of W:Mo ratio on the shift of excitation and emission spectra in the scheelite-powellite series. *Amer. Mineral.* 73, 1145–1154.
- USPENSKY, E.I. (1994): A new kind of X-ray luminescence method for studies on REE distributions in Native scheelites. *Book of abstracts, 16th meeting of the International Mineralogical Association*, Pisa, 4–9 septembre 1994, 418.
- USPENSKY, E.I. and ALESHIN, A. (1993): Patterns of scheelite mineralization in the Muruntau gold deposit, Uzbekistan. *International Geology Review* 35, 1037–1051.
- USPENSKY, E.I., NOVGORODOVA, M.I., MINEYEVA, R.M., SPERANSKIY, A.V., BERSHOV, L.V. and GAFT, M.L. (1990): Europium anomaly in scheelite from gold deposits. *Transactions (Doklady) of the USSR Academy of Sciences, Earth Sciences section* 27, 179–182.
- WENGER, C. (1983): *Mineralogisch-Petrographische Untersuchungen im Val Pirocca (Malcantone); Scheelit-Prospektion im Sotto Ceneri und Untersuchungen der Scheelitvorkommen*. Unpublished Diploma Thesis, University of Bern.
- WENGER, C. (1987): *Scheelitvorkommen im Sottoceneri. Allgemeines zur Geochemie und Lagerstättenkunde Wolframs*. Ph.D. Thesis, University of Bern.
- WOODTLI, R., JAFFÉ, F., VON RAUMER, J. and DELLA VALLE, G. (1987): Prospektion minière en Valais: le projet uromine. *Matériaux pour la géologie de la Suisse, Série géotechnique* Liv. 72, 1–180.
- WUTZLER, B. (1983): *Geologisch-lagerstättenkundliche Untersuchungen am Mont Chemin (Nördöstliches Mont Blanc-Massiv)*. *Clausthaler geol. Abh.* 42.
- ZUFFARDI, P. (1989): Italy. In: DUNNING, F.W. and EVANS, A.M. (eds): *Mineral deposits of Europe*. v. 4/5: Southwest and Eastern Europe, with Iceland. The Institution of Mining and Metallurgy, The Mineralogical Society, London.
- ZURBRIGGEN, R. (1996): Crustal genesis and uplift history of the Strona-Ceneri zone (Southern Alps): a combined petrological, structural, geochemical, isotopic, and paleomagnetic study. Ph.D. Thesis, University of Bern.

Received July 1, 1997; revision accepted December 12, 1997.